

# Evaluating the Effectiveness and Robustness of Visual Similarity-based Phishing Detection Models

Fujiao Ji<sup>1</sup> Kiho Lee<sup>1</sup> Hyungjoon Koo<sup>2</sup> Wenhao You<sup>3</sup> Euijin Choo<sup>3</sup> Hyoungshick Kim<sup>2</sup> Doowon Kim<sup>1</sup>

<sup>1</sup>*University of Tennessee, Knoxville* <sup>2</sup>*Sungkyunkwan University* <sup>3</sup>*University of Alberta*

## ABSTRACT

Phishing attacks pose a significant threat to Internet users, with cybercriminals elaborately replicating the visual appearance of legitimate websites to deceive victims. Visual similarity-based detection systems have emerged as an effective countermeasure, but their effectiveness and robustness in real-world scenarios have been unexplored. In this paper, we comprehensively scrutinize and evaluate state-of-the-art visual similarity-based anti-phishing models using a large-scale dataset of 450K real-world phishing websites. Our analysis reveals that while certain models maintain high accuracy, others exhibit notably lower performance than results on curated datasets, highlighting the importance of real-world evaluation. In addition, we observe the real-world tactic of manipulating visual components that phishing attackers employ to circumvent the detection systems. To assess the resilience of existing models against adversarial attacks and robustness, we apply visible and perturbation-based manipulations to website logos, which adversaries typically target. We then evaluate the models' robustness in handling these adversarial samples. Our findings reveal vulnerabilities in several models, emphasizing the need for more robust visual similarity techniques capable of withstanding sophisticated evasion attempts. We provide actionable insights for enhancing the security of phishing defense systems, encouraging proactive actions. To the best of our knowledge, this work represents the first large-scale, systematic evaluation of visual similarity-based models for phishing detection in real-world settings, necessitating the development of more effective and robust defenses.

## 1 INTRODUCTION

Phishing attacks currently pose a significant security threat to billions of Internet users [1, 2]. Cybercriminals fabricate deceptive websites mirroring authentic ones, often targeting online financial institutions (e.g., PayPal) or social media (e.g., Facebook). This aims to deceive users into disclosing sensitive information, such as login credentials or credit card information. With meticulous attention to detail, these adversaries carefully replicate the appearance of genuine target brand websites by incorporating identical or closely resembling logos, fonts, layouts, and other visual elements to create a convincing illusion.

In the ongoing battle against phishing attacks, the anti-phishing ecosystem constantly strives to thwart these malicious activities. As this effort involves two primary aspects of phishing websites, namely, (1) URLs and (2) client-side resources of webpages (*i.e.*, the appearance of phishing websites), the defense systems rely on analyzing these aspects to determine whether a website is involved in phishing activities. Lately, visual similarity-based defense mechanisms [3–8] have emerged as one of the most effective and potent tools in the arsenal of defense mechanisms. The mechanisms are

required to curate a list of references of visual components, including screenshots or logos, for popular brands. They can efficiently flag potential phishing attempts by detecting fraudulent sites that exhibit a high degree of visual resemblance to well-known target brands (e.g., Facebook or PayPal) but with different domains.

Although visual similarity-based defense mechanisms have individually shown promising results in varying contexts [3–6, 8], their overall effectiveness and robustness in real-world scenarios remain unexplored. Prior evaluations were conducted in controlled experimental settings, such as reference brand lists used for training, limiting the capture of the complexities of real-world phishing campaigns. A notable gap arises from the absence of (1) large-scale evaluations across multiple detectors under uniform and fair conditions, (2) in-depth analyses of influential factors affecting outcomes for adversarial attacks, as shown in Figure 1, and (3) efforts to identify weaknesses in terms of each influential factor. This restricts the provision of more actionable and concrete recommendations for the proposed approaches.

Our work aims to bridge these gaps by comprehensively evaluating prominent visual similarity-based models with a large-scale dataset of real-world phishing websites. We also conduct experiments on the robustness of those models. To this end, we raise the following research questions: **RQ1:** Do visual similarity-based anti-phishing mechanisms maintain their *effectiveness* and *robustness* against real-world phishing attacks under the same experimental settings? **RQ2:** Are visual similarity-based anti-phishing mechanisms sufficiently resilient against adversarial strategies that manipulate visual components to evade detection?

To address RQ1, we conduct a systematic performance assessment of state-of-the-art models on a large-scale dataset comprising 450K real-world phishing websites. Our analysis reveals that while certain models, such as PhishIntention [4] and PhishZoo [8], maintain high accuracy, others exhibit notably lower performance than reported results on curated datasets. This discrepancy highlights the importance of evaluating models on real-world data for a precise evaluation of their efficacy. Furthermore, our study identifies specific weaknesses in each model, providing valuable insights and highlighting key areas that require improvement to enhance the robustness and reliability of visual similarity-based anti-phishing models. For example, our finding shows that TF-IDF (Term Frequency-Inverse Document Frequency) [9] from PhishZoo [8], which filters candidate keywords from HTML and URLs, restricts overall performance. This is because TF-IDF evaluates the frequency of a word within the HTML and measures its importance across the HTML. However, HTML contains a lot of ‘stop words’ which can let the methods choose non-content terms (e.g., ‘the’, ‘of’).

To address RQ2, we semi-manually apply various adversarial perturbations to visual elements such as logos and evaluate the robustness of target models. Our findings show the weaknesses in

**PhishIntention** [4] and **VisualPhishNet** [5], highlighting the need for more robust visual similarity techniques capable of withstanding adversarial evasion attempts. Particularly, visible manipulations significantly impact logo-based models. Our evaluation provides valuable insights into building a reliable and resilient model against adversarial attacks and sophisticated evasion strategies.

The following summarizes our contributions.

- We conduct the first comprehensive study using a large-scale dataset of over 450K real-world phishing websites to evaluate six visual similarity-based anti-phishing systems. Our findings suggest that these systems are less effective in real-world scenarios, indicating significant performance degradation (20.7%) compared to their results on their curated datasets.
- We generate over 7,119 adversarial samples using 14 types of visible manipulations and 5 adversarial perturbations on phishing web pages, reflecting real-world phishing patterns and sophisticated attacks. Our results show critical limitations in visual similarity-based phishing detection models against adversarial samples. We will provide our dataset as a benchmark for future research.
- Based on our findings, we recommend several strategies to improve the effectiveness and robustness of visual similarity-based anti-phishing mechanisms. These include integrating text recognition with visual analysis and using preprocessing techniques such as scaling and denoising to minimize the impacts of adversarial perturbations.

## 2 BACKGROUND

**Phishing Campaigns.** Phishing is a type of social engineering attack in which attackers try to trick victims into disclosing sensitive information such as passwords and credit card details. A generic phishing attack involves fraudulent websites that mimic the appearance of legitimate websites familiar to intended victims. Then, attackers distribute deceptive messages designed to convince victims that they are interacting with trustworthy entities. Those who are successfully lured will visit the phishing website and undoubtedly pass on their private information. Typically, such stolen information could be misused for further fraud or crimes.

**URL-based Phishing Detection Systems.** URL-based detection systems are one of the most common approaches to detecting phishing attacks. These systems identify phishing sites by analyzing the features of the URLs. A prominent example of a URL-based detection method is the blocklist-based defense mechanism (e.g., Google Safe Browsing [10]). Known phishing websites' URLs are compiled into blocklists, which are then utilized by this approach. When users attempt to access specific URLs, the blocklist-based system performs a database lookup to verify if those URLs are present in the blocklist. If the URLs are found in the database, users are prevented from accessing those sites. This approach offers low false positive rates and enables high-speed URL verification on the client side, making it an efficient and reliable line of defense. However, the blocklist-based approach inherently suffers from a time delay between the deployment of a phishing website and its eventual inclusion in the blocklist databases. During this critical window, unsuspecting users may fall victim to the phishing attempt before the site is identified and blocked. Notably, Adam *et al.* [11] highlighted



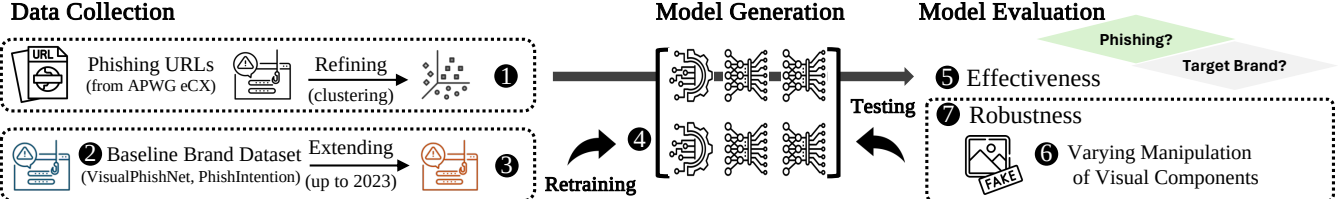
(a) Original Login Form of Face-book.com (b) Adversarial Manipulation of Logo Text (Upper Case and Font)

Figure 1: Examples of Original Login Form and Adversarial Manipulation. An attacker changes the logo text ('facebook') to its upper case ('FACEBOOK') and its font as well. Note that the (b) example is found in our real-world phishing dataset.

that over 50% of victims have already visited before phishing URLs are blocked. To protect users from newly generated phishing URLs, some detection approaches [12–17] employ machine learning or deep learning models trained on various URL features to detect phishing websites. However, relying solely on URLs for training models is insufficient, as they provide limited information about websites' content, structure, or visual appearance, which are crucial for accurate phishing detection.

**Visual Similarity-based Phishing Detection Systems.** To overcome URL-based detection methods, a design focus has been shifted toward the visual components of phishing websites (e.g., screenshots and logos). For instance, Anthony *et al.* [6] measure the Earth Mover's Distance (EMD) [18], Afroz *et al.* [8] use the Scale-Invariant Feature Transform (SIFT) feature for image-matching. Liu *et al.* [19] assess block, layout, and style similarity. Lately, with the advancement of deep learning, researchers have adopted deep learning-based methods for capturing image features and comparing similarities. For example, **VisualPhishNet** [5] utilizes triplet convolutional neural networks to learn visual similarities between screenshots of webpages from the same website, while **Phishepedia** and **PhishIntention** incorporate Faster-RCNN [20] for logo recognition and the Siamese architecture for similarity comparison.

**Adversarial Visual Component Manipulation Attacks.** One of the crucial aspects of phishing websites is their visual appearance, which directly influences the target user's perception. Phishing campaigns aim to replicate the appearance of legitimate brand websites to deceive potential victims. Consequently, anti-phishing mechanisms attempt to identify phishing attacks using visual similarity between phishing websites and their legitimate target brand websites. From the phishing attackers' perspective, they seek to evade anti-phishing systems by manipulating visual components (e.g., logo images) as a new tactic. However, adversaries must ensure that manipulated visual components effectively deceive potential victims while also bypassing phishing defense systems. Particularly, Lee *et al.* [22] introduce an adversarial learning-based framework based on perturbation vectors, demonstrating that target logos applied with these vectors can bypass phishing detectors while remaining undetectable to human eyes. Figure 1-(b) is an example of an adversarial visual component (logo) manipulation where an adversary changes the text logo ('facebook') to its upper case ('FACEBOOK'), and also the text font as well. Note that this example is found in our real-world phishing dataset.



**Figure 2: Overview of Our Experiment.** First, we collect a real-world phishing dataset (*i.e.*, screenshots and HTML files) with URLs from APWG eCX. Then, we refine the dataset by filtering out the pages that involve errors (*e.g.*, HTTP 404) or CAPTCHA (❶); Section 4.2). Note that we use the APWG dataset for testing model purpose alone. Second, we prepare two additional datasets: the baseline from combining PhishIntention [4] with VisualPhishNet [5] and the extended one with more reference brands (❷ and ❸; See Table 1). Next, we carefully select six state-of-the-art visual similarity-based anti-phishing techniques [3–6, 8, 21] and re-train them with these datasets (❹). Third, we systematically evaluate the models with the APWG dataset (❺; Section 4.4). Lastly, we manipulate visual components (*e.g.*, logo images) with varying transformations (❻; Section 4.5), assessing the robustness of the above models (❻).

### 3 PROBLEM STATEMENT

The *visual similarity-based* defense mechanisms [3–8], which compare the visual features of a website with those of a known legitimate website, have emerged as effective phishing detectors. They rely on the insight that phishing pages visually mimic legitimate websites, especially by replicating logos, the most recognizable brand elements users rely on to identify a website’s legitimacy. However, the effectiveness and robustness of these methods against real-world phishing attacks, especially those involving sophisticated logo manipulations, remains underexplored, leaving a critical gap in current defenses. To bridge this gap, we comprehensively evaluate prominent visual similarity-based anti-phishing models using a large-scale real-world phishing dataset.

Moreover, to evaluate the models’ robustness against this new tactic, We semi-manually manipulate visual components (logo images) according to our predefined rules (Table 6), as shown in Table 2 and Figure 4. Then, we evaluate the robustness of the models using our manipulated visual components. By testing the models on this dataset, we aim to uncover their strengths and weaknesses in detecting adaptive adversaries. Our study comprehensively analyzes the real-world effectiveness and robustness of visual similarity-based phishing detection models, offering insights for developing more resilient defenses against evolving phishing tactics. Our study aims to:

- Assess the effectiveness of current visual similarity-based models against real-world phishing attacks.
- Identify the root causes of the models’ failures in classifying phishing websites.
- Investigate a new phishing tactic that manipulates visual components like logo images to circumvent existing visual similarity-based models.

## 4 COMPREHENSIVE EVALUATION DESIGN

### 4.1 Overview of Evaluation Methodology

The primary objective of our study is to comprehensively evaluate the effectiveness and robustness of state-of-the-art visual similarity-based phishing detection models using a large-scale dataset of real-world phishing websites. As the overview of our experiments is illustrated in Figure 2, our methodology includes the following key steps. *First*, we develop a web crawler that periodically (every 10

minutes) collects the screenshots and client-side resources (*e.g.*, HTML) of real-world phishing websites using URLs reported by APWG eCX [23] (❶). Then, we refine our collected dataset by removing unnecessary data (*e.g.*, error pages) via clustering screenshots. More information will be described in Section 4.2.

*Second*, we carefully select six visual similarity-based phishing defense models (❷). Specifically, we begin by selecting visual similarity-based model candidates presented at major security and machine learning conferences (*e.g.*, USENIX Security and CVPR), as described in Table 7. From the candidates, we choose models with publicly available codes and datasets used for the models. Then, based on the model type (a deep learning-based or machine learning-based model) and model input type (like screenshots and logos), we finally select six models for our evaluation. More information will be described in Section 4.3.

*Third*, before evaluating the effectiveness and robustness of the six models, to ensure fairness in our evaluation, we begin by *re-training* models under the same settings—the same phishing target brand reference datasets (❸). Specifically, to achieve more accurate evaluations on our collected real-world phishing (*i.e.*, APWG) dataset, we re-train models with the two types of distinct target brand reference list datasets under the same settings, yielding two variations of models. Note that the re-training step is crucial as the existing models were trained under different conditions and with varying phishing target brand reference lists (*i.e.*, training datasets), which can substantially impact the evaluation outcomes. For example, a model might not learn about a specific target brand while our testing dataset includes it. This inequality leads to biased results, undermining the fairness of the evaluation.

In our re-training process, we assemble two distinct training datasets: (1) the baseline phishing target brand reference dataset from public sources ( $D_{tr1}$ ), and (2) our extended reference dataset ( $D_{tr2}$ ), which is augmented with additional data. Table 1-(a) shows the statistics of our collected re-training datasets. For (1) the baseline dataset ( $D_{tr1}$ ), we employ the original PhishIntention dataset to re-train logo-based anti-phishing models and the original VisualPhishNet dataset for models relying on screenshots. For (2) the extended reference dataset ( $D_{tr2}$ ), we extend  $D_{tr1}$  by adding new logo images or screenshots from the same target brand websites because  $D_{tr1}$  contains old logos and screenshots of target brand

websites. To achieve this, we utilize the Internet Archive (<https://archive.org/>) to manually collect new logo images and screenshots observed between 2016 and 2023 (seven years). More information will be described in Section 4.4.

Fourth, we evaluate the effectiveness of the six models using our real-world phishing datasets (4). We curate two types of datasets for evaluation:  $D_{ts1}$  and  $D_{ts2}$  as shown in Table 1-(b). The  $D_{ts1}$  dataset is curated by identifying common brands between the reference brand list ( $D_{tr1}$ ) and our collected phishing websites dataset ( $D_{ts2}$ ). This evaluation helps us better understand the models' effectiveness for specifically targeted brands learned by the models. The  $D_{ts2}$  dataset is curated from our collected real-world phishing dataset that includes brands not learned by the models. This helps us better understand models' effectiveness in real-world scenarios, as the real world contains brands not learned by the models. By comparing the results from  $D_{ts1}$ , we can assess the influence of these unlearned data on the models.

After identifying the root failures of the models (e.g., changing the text logo to its upper case, as shown in Figure 1-(b)), we attempt to understand why the models fail to classify specific phishing attacks (5). We address RQ2 by designing another experiment where we manipulate visual components (e.g., logo images) of phishing websites in two ways (6): (1) visible manipulation techniques (e.g., changing logo color or location) and (2) perturbation-based adversarial manipulation techniques (i.e., perturbing logos). Table 2 illustrates the examples of the manipulations in our experiment. Then, we evaluate the robustness of the models using the manipulated dataset and identify their failures (7). We will further discuss the details in Section 4.5.

## 4.2 Real-world Phishing Dataset Collection

We collect real-world phishing websites using APWG eCX to evaluate anti-phishing detection models, which helps us uncover common patterns and unique approaches phishing attackers employ.

**Web Crawler Design.** We design a web crawler that regularly (every 10 minutes) gathers (1) client-side resources (e.g., logo images, HTML, etc.) of phishing websites and captures (2) screenshots of phishing websites. We implement the web crawler using **Google Selenium Chrome WebDriver** [24] because it can simulate real user interactions with phishing websites, which includes fully loading and rendering all client-side resources (e.g., JavaScript, CSS, images, etc.) on the webpages. This capability provides a comprehensive view of the phishing web pages, as the crawler captures the complete rendered web pages, similar to how a human user would experience them. Additionally, **Selenium Chrome WebDriver** can assist in evading anti-bot techniques employed by phishing websites. These techniques attempt to assess whether the visitor is a genuine user or an automated bot and block access if identified as a bot [25, 26]. The **Chrome WebDriver**'s ability to mimic real user interactions might help bypass such anti-bot techniques [25, 26].

**Our Initially-collected Dataset.** Our crawler is fed phishing URLs from APWG eCrime Exchange (eCX)[23], which have been deployed in the real world. APWG eCX is utilized by prior work [27–31] to gain deeper insights into the phishing attack ecosystem because it is one of the largest repositories of reported phishing attacks and provides highly reliable data on real-world phishing incidents. Specifically, as shown in Table 1b, our crawler receives 15,747,193

**Table 1: Training and Testing Reference List Dataset. Training datasets are used for re-training the models.**

**(a) Training Dataset: Phishing Target Brand Reference Lists.**

	Definition	Dataset Source	Target Model	# Brand	# Image
$D_{tr1}$	Baseline Ref.	PhishIntention [4] VisualPhishNet [5]	L-based S-based	277 (B) 155 (B) 155 (P)	3,064 9,363 (B) 1,193 (P)
	Extended Ref.	Extended Logo Extended Screenshot	L-based S-based	277 (B) 277 (B) 213 (P)	3,167 9,633 (B) 1,179 (P)
<b>L-based</b> = Logo-based models; <b>S-based</b> = Screenshot-based models; <b>B</b> = Benign; <b>P</b> = Phishing.					

**(b) Testing Dataset: Collected Real-world Phishing Websites.**

	Type	# URL	# Domain	# Brand	# Cluster
$D_{ts1}$	Only-Learned-Brand Dataset	312,355	104,813	110	2,797
$D_{ts2}$	All-Brand Dataset	451,514	163,864	270	4,190

(15.7M) real-world phishing URLs from July 2021 to July 2023 (25 months) and successfully accessed 6,118,654 (6.1M) phishing websites. Although our crawler attempts to access the reported phishing websites within 10 minutes, 61.1% of websites (out of 15.7M) are inaccessible due to server shutdowns or network errors such as DNS resolving errors. Our crawlers successfully collect client-side resources and take screenshots of 6.1M phishing websites.

**Internal Access Errors in Our Dataset.** Our crawler occasionally encounters internal access errors even after successfully accessing phishing URLs and their corresponding web servers. These errors can arise from issues within the internal web server, such as 404 errors (i.e., page not found) and internal DB connection errors. Additionally, other errors may be caused by blocking or evasion techniques employed by the websites, such as CAPTCHAs. These internal errors could introduce bias in evaluating anti-phishing mechanisms. For example, CAPTCHA pages or 404 error pages may differ from target legitimate websites, and the existing anti-phishing mechanisms may erroneously classify the screenshots of these internal errors as legitimate websites. To address this issue, we employ a thorough filtering process using a *clustering* technique. This technique helps us identify and remove the internal error pages from our collected dataset, ensuring that our evaluation is based on the intended phishing website content rather than other internal access errors. By removing these internal access errors through clustering, we aim to mitigate potential biases and ensure the accuracy and reliability of our analysis on anti-phishing mechanisms.

**Removing Errors from Our Dataset.** We first cluster our 6,125,810 (6.1M) screenshots to identify internal error web pages and then remove them from our collected datasets. We utilize Fastdup [32], an unsupervised open-source tool designed for analyzing image datasets. This tool is particularly effective in identifying duplicates, outliers, and clusters of related images within datasets, even when dealing with high contamination rates. Through this process, we identify a total of 407,926 clusters. We define a cluster as such, even if it contains only one image. The cluster sizes vary, with the maximum, minimum, mean, and median sizes being 1,404,549, 1, 15, and 1 screenshot(s), respectively. Then, for our manual analysis, we select only clusters that contain 20 or more screenshots, which represent 90.00% of the total 6.1M screenshots with 6,885 clusters. We manually identify error pages and target brands from these 6,885 clusters, as we can pick one sample and identify it from each cluster. After removing the error pages, there remain 4,190 clusters with 270 brands and 2,160,933 screenshots.

**Final Dataset for Evaluation.** Analyzing this dataset directly poses challenges due to the fact that a small percentage (2.77%) of clusters (*i.e.*, merged brands) hold the majority (97.23%) of total screenshots. This distribution makes the evaluation process time-consuming and susceptible to bias. Therefore, to ensure fairness in evaluation, we randomly select 1,000 samples for each cluster (if the number of screenshots in the cluster is lower than 1,000, all of them are selected for evaluation). This process results in a total of 451,514 samples with 270 brands and 4,190 clusters, as  $D_{ts2}$  in Table 1b.

Furthermore, when evaluating the models using the  $D_{ts2}$  dataset, this dataset may include some brands that are not present in the training dataset, meaning the brands are not learned by models. We identify 110 common brands between  $D_{tr1}$  and  $D_{ts2}$ . This dataset, called  $D_{ts2}$ , includes 312K samples with 110 brands. In summary, the  $D_{ts1}$  dataset is used for assessing the models' actual effectiveness with learned brands, while the  $D_{ts2}$  dataset is to better understand the models' performance in real-world scenarios and to examine the impact of data on unlearned brands.

### 4.3 Target Model Selection

We carefully select representative models of visual similarity-based anti-phishing techniques for our comprehensive evaluations. *First*, to identify model candidates, we initially search for visual detection models using some keywords, such as ‘anti-phishing,’ ‘phishing detection,’ and ‘visual-based similarity,’ at the Big Four security conferences, top computer vision, and top machine learning conferences. We summarize our model candidates in Table 7 of Appendix A.1.

*Second*, from these candidates, we choose models with available published or re-implemented codes to ensure fidelity to the original papers. Specifically, our selection includes two deep learning models, **PhishIntention** [4] and **Phishpedia** [3], specifically designed for detecting phishing mainly through logo images. Additionally, we include **VisualPhishNet** [5], a deep-learning model that detects phishing using screenshots. To provide a comprehensive comparison, we incorporate two traditional machine learning approaches, **EMD** (Earth Mover’s Distance) [6] for screenshot-based phishing detection and **PhishZoo** [8] for logo-based detection. Finally, we include **Involution** [33], a model not specifically tailored for phishing detection, to provide a broader baseline for comparison. Detailed model information can refer to Appendix A.2.

### 4.4 Re-training Models & Evaluation Plan

We aim to rigorously evaluate the effectiveness of six selected visual similarity-based anti-phishing models, comprising four deep-learning models and two machine-learning models, with our extensive dataset of real-world phishing websites. Initially, it is important to note that not all models are publicly available; only source code is accessible, necessitating the training of the models using specific datasets. Moreover, training under varying conditions and with diverse reference lists can significantly impact the evaluation outcomes. Additionally, the presence of either outdated or new visual elements, such as logo images or login forms, can profoundly affect model performance, as these elements might not have been adequately captured during initial training. For example, updates to Facebook’s login form, user interface, or icons could potentially adversely impact the model’s performance. To ensure a more equitable and cautious approach in evaluations and model performance

comparisons, we *re-train* the models under uniform conditions, taking these factors into account.

**Two Variants of Re-trained Models.** Our objective is to develop two variants of re-trained models. The distinction between the two variants lies in the reference lists used: (1) the baseline phishing target brand reference dataset ( $D_{tr1}$ ) and (2) our expanded reference dataset ( $D_{tr2}$ ), as detailed in Table 1-(a). For  $D_{tr1}$ , we utilize the **PhishIntention** logo dataset and their original datasets for training logo-based anti-phishing models and the **VisualPhishNet** screenshot dataset for models that depend on screenshots. Note that the **PhishIntention** screenshot dataset is not used for training screenshot-based methods due to the need for phishing information during the **VisualPhishNet** training phase. To maintain consistency in brand knowledge across models, we use the **PhishIntention** screenshot dataset as a reference list during testing.

## 4.5 Manipulating Visual Component (Logo)

Through our evaluation experiment, we analyze the manipulation tactics employed by phishing attackers. We find that there are three primary components typically exploited by adversaries in phishing attacks, including logos, pop-ups, and login forms, as presented in Appendix A.3. Upon randomly selecting manipulated images from the failure results, we discern that logo component manipulations are prevalent strategies adversaries employ to circumvent the detection mechanisms. Furthermore, the logo is an important component for both users and detection mechanisms to recognize the target brand. Consequently, in this study, our primary focus is on logo manipulation.

**4.5.1 Manipulation Methods.** Phishing attackers not only aim to mimic legitimate target brand websites to deceive potential victims closely but also aim to evade detection by anti-phishing systems, particularly those based on visual similarity. To achieve this, they have developed various adversarial visual component manipulation strategies. We can broadly categorize such strategies into (1) visible manipulation techniques and (2) perturbation-based adversarial manipulation techniques.

**Visible Manipulation Methods.** The visible manipulation techniques involve substantial, noticeable changes to the original visual appearance, such as altering the image color [36], text [37], and UI design patterns [38]. For instance, during such attacks, visual components like logos (*e.g.*, changing the ‘facebook’ logo’s font and converting the letters to uppercase) are manipulated, as illustrated in Figure 1. Based on the failure samples discussed in Section 5, we identify the types of manipulations used by adversaries and carefully design 13 manipulations that affect visual appearance in this category and craft samples corresponding to these manipulations. Specifically, we use ‘remove.bg’ [39] to eliminate the background of logos for different manipulations. If users are not looking at the logos carefully, they readily overlook it and can be readily lured. The manipulations and crafted examples are shown in Table 2. Note that we do not combine more than two visible manipulation ways. **Perturbation-based Manipulation Methods.** On the other hand, (2) perturbation-based adversarial manipulation techniques introduce subtle manipulations that are difficult for humans to detect

**Table 2: Example and Description of Visible Manipulation Methods.**

Example	Method Description	Example	Method Description
	<b>Original:</b> This is the original logo cropped from the “YouTube” original website.		<b>Flipping:</b> We flip the logo vertically or horizontally. This differs from “Rotation,” where we control the rotation to a limited small degree.
	<b>Color:</b> We identify the logo in the screenshot and then change the color. In this example, we change it from the original red to blue, but the attacker could use any other predefined color.		<b>Ratio:</b> We randomly modify the height-to-width ratio of the logo. In the example shown, the proportions change to the original proportions minus 0.08.
	<b>Rotation:</b> We rotate the logo in small increments clockwise or counterclockwise, and fill the empty area created by the rotation with the color of the surrounding background. In this example, it is rotated clockwise by 1 degree.		<b>Combination:</b> We randomly select a second logo from a set of 110 different target brands and place it either above, below, or to the left of the original logo in the screenshot. For example, the “YouTube” is combined with “Spark NZ.”
	<b>Replacement:</b> We replace the original logo with a logo randomly selected from 110 brands. For example, the login form is still “YouTube,” but the logo is replaced with “Raiffeisen Bank.”		<b>Scaling:</b> We resize the logo, increasing both the length and width to 1.1 times the original size, and then place the resized logo in the screenshot of “Deletion.”
	<b>Deletion:</b> We remove the logo from the screenshot and fill the area with the surrounding background color. The region detector may identify other components (“sign in”) as the logo.		<b>Blurring:</b> We add Gaussian blurring with kernel size 9 to the entire screenshot image, including the logo and the background, by the “OpenCV” Python package.
	<b>Location:</b> We move the position of the logo horizontally within the screenshot and fill the original logo position with the surrounding background color. For example, the logo is moved from the top left to the bottom left.		<b>Division:</b> We use only one of the elements of the logo (either icon or text) and fill the rest with the surrounding color. For example, we keep the icon and remove the text “YouTube.”
	<b>Font:</b> We use a font identification tool [34] to find similar fonts. Then, we generate text in those fonts and replace the original logo. We also use the SRNet [35] to generate text logos while keeping the background context, font style, and color.		<b>Case:</b> We find a font that looks similar to the text logo. Then, we change the capitalization of the text to make all letters capitalized, all letters lowercase, or just the first letter capitalized. For example, “YouTube” is transformed to “YOUTUBE” with all letters in uppercase.

visually, such as introducing small perturbations [40–43] or generating adversarial samples to attack visual similarity-based anti-phishing mechanisms. A recent study [22] introduced a perturbation-based adversarial manipulation model targeting visual similarity-based anti-phishing mechanisms, demonstrating the ability to generate perturbed logos that significantly degrade the detection rates of state-of-the-art phishing detectors. In this scenario, the manipulation methods can be categorized into two: (a) white-box attack and (b) black-box attack. The crafted examples are shown in Appendix 4.

For the (a) white-box attack methods, the Fast Gradient Sign Method (FGSM) [41] perturbs the data in a single step by using an imperceptibly small vector whose elements are equal to the sign of the elements of the gradient of the cost function with respect to the input. Projected Gradient Descent (PGD) [42] suggests an iterative version of FGSM with a random start, which is much closer to the optimal adversarial example. Carlini & Wagner (CW) attack [43] constructs three new attacks for the three distance metrics.

For (b) the black-box attack, we follow the recent work [22] and utilize generative adversarial perturbations to develop adversarial logos. Specifically, the model employs the trained Vision Transformer (ViT) [44] and Swin Transformer [45] models as Discriminators and a Deep Residual Network with six residual blocks (ResNet-6) as the foundational architecture of the Generator. We

train the attack models on the extended logo dataset in Table 1a. Furthermore, we also replace the original logo position with the modified one on the screenshots, ensuring a seamless integration into the visual context.

**4.5.2 Evaluation Plan.** Recall that all models used to evaluate robustness are trained on the ‘Extended Ref.’ ( $D_{tr2}$ ) or baseline ( $D_{tr1}$ ) datasets along with the original needed datasets. To get more accurate results, we focus on only the learned 110 brands ( $D_{ts1}$ ) for evaluation. To create a diverse set of test cases, we apply ‘typosquatting’ techniques to generate various squatted versions of the original URLs for each phishing manipulation technique. We manually collect the URLs of the login page or main page domain of each website, and employ *typosquatter* [46] to generate various domain typos to test URLs’ impact on models as well. Finally, the total dataset contains 110 brands with 6,528 screenshots, benign URLs with 110, and squatted URLs with 1,321. These squatted URLs are then paired with their corresponding altered visual images to curate the phishing testing dataset for evaluation.

## 5 EVALUATION IN REAL-WORLD SETTINGS

We evaluate the effectiveness of the six models with our real-world phishing dataset, employing two criteria: phishing detection rate and phishing brand identification. We further analyze the root

**Table 3: Phishing Detection Results on 312,355 ( $D_{ts1}$ ) and 451,514 ( $D_{ts2}$ ) testing samples from APWG. Phishing Brand Identification Results on 312,355 ( $D_{ts1}$ ). The bold numbers denote the better detection or identification rate in these six models.**

Model	Phishing Detection				Phishing Brand Identification (with $D_{ts1}$ )					
	Only-Learned Brands (312,355) $D_{ts1}$		All Brands (451,514) $D_{ts2}$		Baseline Ref. ( $D_{tr1}$ )			Ext. Ref. ( $D_{tr2}$ )		
	Baseline ( $D_{tr1}$ )	Ext. Ref. ( $D_{tr2}$ )	Baseline ( $D_{tr1}$ )	Ext. Ref. ( $D_{tr2}$ )	$I_{tp}^1$	$I_{tp}/N_p^2$	$I_{tp}/N_{tp}^3$	$I_{tp}^1$	$I_{tp}/N_p^2$	$I_{tp}/N_{tp}^3$
PhishIntention	204,880 (65.59%)	206,846 (66.22%)	235,838 (52.23%)	237,861 (52.68%)	200,134	64.07%	97.68%	202,123	64.71%	97.72%
Phishpedia	232,572 (74.46%)	<b>274,779 (87.97%)</b>	275,292 (60.97%)	318,196 (70.47%)	222,860	71.34%	95.82%	<b>265,627</b>	<b>85.04%</b>	96.67%
Involution	<b>253,965 (81.31%)</b>	264,782 (84.77%)	289,058 (64.02%)	301,035 (66.67%)	<b>253,090</b>	<b>81.03%</b>	<b>99.66%</b>	263,835	84.47%	<b>99.64%</b>
PhishZoo	241,206 (77.22%)	269,748 (86.36%)	<b>353,292 (78.25%)</b>	<b>389,585 (86.28%)</b>	30,829	9.86%	12.78%	89,724	28.73%	33.26%
VisualPhishNet	122,106 (39.09%)	126,762 (40.58%)	181,177 (40.13%)	186,606 (41.33%)	81,119	25.97%	66.43%	83,697	26.80%	66.03%
EMD	95,632 (30.62%)	97,880 (31.34%)	133,241 (29.51%)	136,697 (30.28%)	22,478	7.20%	23.50%	22,426	7.18%	22.91%

<sup>1</sup> $I_{tp}$  = The number of phishing samples correctly identified; <sup>2</sup> $I_{tp}/N_p$  = The phishing target brand identification rate out of the total phishing testing samples;<sup>3</sup> $I_{tp}/N_{tp}$  = The phishing target brand identification rate out of the only samples detected as phishing by each model.

cause of failures in phishing detection that we observe from our evaluation (*i.e.*, misclassification).

**Evaluation Settings.** We leverage ‘Only-Learned-Brand Dataset ( $D_{tr1}$ )’ and ‘All-Brand Dataset ( $D_{ts2}$ ) Dataset’ in Table 1-(b) to evaluate our re-trained models. We define  $N_p$  as the number of phishing testing samples,  $N_{tp}$  as the number of phishing samples predicted as phishing, and the number of correctly identified target brands for reported phishing samples as  $I_{tp}$ . Then the phishing detection accuracy rate is  $N_{tp}/N_p$ , the phishing identification rate out of the total testing samples is  $I_{tp}/N_p$ , the phishing identification rate out of the reported as phishing is  $I_{tp}/N_{tp}$ .

**Thresholds.** Threshold values, playing a crucial role in our phishing detection process, are obtained by testing on evaluation dataset in the prior work [4] and further checked with their thresholds. Specifically, we set the thresholds as 0.83, 0.83, 40, 1, 0.94, and 0.7 for PhishIntention [4], Phishpedia [3], PhishZoo [8], VisualPhishNet [5], EMD [6], and Involution [33], respectively, to identify potential phishing instances effectively.

## 5.1 Detection Effectiveness Result

Phishing detection refers to a model’s capability to classify websites as either phishing or legitimate. The results are presented in Table 3. Our findings highlight the crucial importance of model design in phishing detection.

**General Performance.** As presented in Table 3, all six models exhibit subpar performance in effectively detecting phishing attacks, contradicting the evaluation results specified in their studies. On average, the six models (trained on the Baseline dataset) are unable to detect approximately 38.62% of the 312,355 only-learned phishing samples ( $D_{ts1}$ ). The six models (trained on the extended reference list dataset) cannot detect approximately 33.8% of the same 312,355 samples. Interestingly, all models trained on the extended brand reference list ( $D_{tr2}$ ) have better detection performance than the ones trained on the baseline dataset ( $D_{tr1}$ ). This indicates that all models are *not* resilient to the new logos and screenshots of the same target brand websites. In other words, despite being trained on previous logos and screenshots, the models fail to recognize new or slightly modified logos, indicating a lack of robustness in their detection capabilities. This vulnerability arises because the methods based on reference lists often rely on the similarity between these lists and the test samples to make decisions. The size of the reference list reflects the extent of the models’ knowledge. If attackers exploit the absence of new logos of certain brands in the reference list, the

models may be easily vulnerable. Specifically, in our training dataset, if the models employ  $D_{tr1}$  for their decision-making process, the vulnerability could stem from the discrepancies  $D_{tr1}$  and  $D_{tr2}$ .

**Takeaway 1:** The comprehensiveness of the target brand reference list significantly impacts the phishing detection model’s performance, with more extensive lists leading to better detection of new phishing websites.

**Learned Vs. Unlearned Testing Dataset.** Recall that the  $D_{ts1}$  dataset only contains learned brands while the  $D_{ts2}$  dataset also contains unlearned brands. Our goal is to investigate the models’ readiness for real-world deployment, where they will face a constant influx of new, unknown phishing websites, and determine their ability to adapt and effectively detect these emerging threats.

As shown in Table 3, the models’ detection performances generally decrease when tested with more challenging scenarios ( $D_{ts2}$ ), such as previously unseen brands and real-world phishing samples, revealing a decline in their effectiveness in these real-world situations. Particularly, the *unlearned* brands have PhishIntention decreased in the detection rate from 66.62% to 52.68% (13.94%↓) with  $D_{tr2}$ , and Phishpedia decreased from 87.97% to 70.47% (17.5%↓), while Involution from 84.77% to 66.67% (18.1%↓).

Interestingly, unlike other logo-based models (PhishIntention, Phishpedia, and Involution), PhishZoo (even though this is a logo-based model) demonstrates robust and consistent performance results, even when encountering previously unseen brands, showcasing its ability to generalize and adapt effectively. For example, with the same ‘Extend Reference list’  $D_{tr2}$ , when testing data change from only-learned brands dataset  $D_{ts1}$  to  $D_{ts2}$ , the detection rate remains stable at around 86%. This is because it uses HTML and URLs to choose candidate keywords and uses the SIFT feature to compare similarity. This contrasts with other logo-based models (PhishIntention, Phishpedia, and Involution), which rely on identifying and comparing logo similarities with their target brand reference list. If either these models fail to recognize the logo or the brand does not appear in the reference list, the similarity score will be lower than the threshold, leading to detection failures (*i.e.*, misclassification).

**Takeaway 2:** Logo-based phishing detection can be more effective in detection when leveraging additional information (*e.g.*, HTML and URLs) and efficient features (*e.g.*, SIFT), which can significantly improve the effectiveness and adaptability in real-world scenarios.

**Baseline Vs. Extended Reference List.** Recall that the Extended Reference List Dataset ( $D_{tr2}$ ) is curated by manually adding more new logos and screenshots of their learned target brands to the baseline dataset ( $D_{tr1}$ ). Typically, the new logos are slightly changed from their prior logos. We observe a significant performance increase in both Phishpedia and PhishZoo models when tested on the 312,355 phishing samples of  $D_{ts1}$ . Specifically, Phishpedia’s accuracy increases from 74.46% to 87.97% (13.51% $\uparrow$ ) while PhishZoo’s accuracy rises from 77.22% to 86.36% (9.14% $\uparrow$ ). These gains are attributed to the extended reference list, which includes recent logo and screenshot updates, highlighting the critical importance of comprehensive and regularly updated logo and screenshot collections in phishing detection model design. In other words, failing to learn new logos or screenshots of even their learned target brands leads to decreased overall performance.

The findings also reveal a potential vulnerability, where attackers can exploit reference-based models using newly updated logos or outdated logos not in the reference list. It is essential to recognize that while increasing reference data (regularly adding new logos) improves detection performance, it also prolongs computing time, presenting a crucial trade-off. This trade-off underscores the need for a strategic model design, where balancing detection efficacy and computational efficiency is vital.

**Takeaway 3:** Training with the extended reference list dataset ( $D_{tr2}$ ), which includes recently updated logos and screenshots, significantly improves the performance of the model. However, the increased computation time associated with processing a large reference dataset requires a careful balance between detection accuracy and efficiency in the model design.

**Model Classification Performance Influence.** PhishZoo, leveraging extracted keywords from URLs and HTML sources to mitigate false positives and employing the SIFT feature to calculate similarity in the target list, has reported promising results in phishing detection tasks. However, our in-depth analysis of the model’s performance on unseen data reveals that the high accuracy initially indicated may be an overestimation of its true capabilities. We reveal that the keyword selection approach based on TF-IDF scoring does not accurately capture brand-specific keywords highly indicative of phishing attempts. Specifically, we identify some examples where common words like ‘the’ and ‘in’ influence classification decisions, exposing a limitation in the feature engineering process.

Furthermore, our findings indicate that screenshot-based reference methods are more stable for brand change for both testing and reference data than logo-based methods, yet their performance is worse. EMD considers distribution to measure the distance between testing samples and the reference list, while VisualPhishNet employs the triplet Convolutional Neural Network to compare two screenshots. Unlike logos, the wide variety of screenshots poses a significant challenge in covering the complete range of variations in the reference target list. Moreover, the results indicate that screenshots not present in the target list but sharing similar designs or features show a high degree of resemblance to those in the target list. This suggests a potential vulnerability in screenshot-based methods due to the vast diversity and similarity among web designs.

**Takeaway 4:** The effectiveness of phishing detection models depends on carefully selecting appropriate features and model architectures. Logo-based methods can be hindered by inaccurate keyword extraction and missing CRP, while screenshot-based methods face challenges due to the diversity and similarity of web designs. Balancing feature choice and model structure is crucial for optimal performance and addressing vulnerabilities.

## 5.2 Phishing Brand Identification Result

Note that phishing target brand identification refers to identifying brand names that phishing attempts target to impersonate. The evaluation is tested on only  $D_{ts1}$  dataset since  $D_{ts2}$  contains unlearned brands. The result is presented in Table 3.

**General Performance.** As illustrated in Table 3, the three models (PhishIntention, Phishpedia, and Involution) exhibit high performance in accurately identifying targeted brands, in contrast to other models which struggle to achieve comparable levels of precision in brand recognition tasks. On average, the six models (trained on the extended reference list dataset  $D_{tr2}$ ) fail to detect about 51% of the 312,355 samples of  $D_{ts1}$  and 57% with Baseline Ref.  $D_{tr2}$ . Interestingly, four models (PhishIntention, Phishpedia, Involution, PhishZoo) trained on the extended brand reference list ( $D_{tr2}$ ) have better identification performance than the ones trained on the baseline dataset ( $D_{tr1}$ ). This highlights a reliance on the phishing brand identification performance on the comprehensiveness of the brand reference list for models. Namely, these models may exhibit degraded performance when encountering brands not represented in their training reference corpus, exposing a limitation in their generalization capabilities beyond the defined brand space. Moreover, the screenshot-based methods (EMD and VisualPhishNet) show insensitivity to changes in the reference list. The average total phishing identification rate of these two models with  $D_{tr1}$  is 16.6% and 16.7% with  $D_{tr2}$ . This is attributed to limited variability in brands within the screenshot brand reference list, which constrains the performance of these models.

Furthermore, we observe that Phishpedia increases the identification rate (out of total) from 71.34% to 85.04% (13.7% $\uparrow$ ) when changing brand reference from ‘Baseline Ref.’ to ‘Extended Ref.’, Involution increases from 81.03% to 84.47% (3.44% $\uparrow$ ), and PhishZoo increases from 9.86% to 28.73% (18.87% $\uparrow$ ). PhishIntention, VisualPhishNet, and EMD are stable even for the reference brand change. It shows that adding logo variation will help Phishpedia and Involution greatly improve the brand identification rate, which means this increased percentage can also be utilized by the adversarial to craft samples that can pass both detection and identification. This can be a threat to these two models. Other models are not sensitive to this change. This is because PhishIntention uses the Credential Part (CRP) of HTML and screenshots in the detection step and filters samples without CRP. This way, the model does not have high detection and identification performance, but this possibility is decreased. However, if attackers can craft the CRP samples, then PhishIntention would have a similar threat to these potential vulnerabilities. Meanwhile, screenshot-based methods are stable because extended screenshot brand reference lists are not enough compared to diverse variations of screenshots for the same brand.

Focusing on the brand identification rate (out of reported as phishing number), we find that once the model can distinguish

testing samples as phishing, **PhishIntention**, **Phishpedia**, and **Involution** methods have a high possibility to recognize target brands based on the logo component, indicating that learned features effectively capture logo information and distinguish between phishing and benign reference logos. Furthermore, this suggests that the reference logo list used by these methods has suitable coverage for the logos in the testing data. In contrast, **PhishZoo** is a logo-based method but has low performance on brand identification. This means that the high detection rate comes from high similarity with other brands. Another possible reason is that keywords selected by the TF-IDF from parsing URLs or HTML introduce some adverse effects on the identification step. **VisualPhishNet** has a higher identification rate than **EMD** because it uses triplet CNN to learn similarities within the same brand while learning differences between different brands. This approach is more effective than the **EMD** method, which may struggle when the distributions of two brands' logos are similar, leading to a low identification rate.

Considering the total performance of phishing detection and phishing brand identification, we observe that **Phishpedia** and **Involution** outperform other methods in detection (except **PhishZoo**) and identification, while **PhishIntention** also demonstrates a reasonable identification rate. This indicates that the features learned by these methods are effective. It also demonstrates that logos play an important role in recognizing the target brand. Based on two tasks' results, **PhishZoo** achieves a lousy result in phishing detection and brand identification because it recognizes the samples as other brands and can be further proved by phishing identification results. The other possible reason is ineffective keyword selection methods. **VisualPhishNet** and **EMD** are working poorly in phishing detection and identification, indicating that these screenshot-based methods are less effective than logo-based ones. They focus on multiple components on the screenshot rather than mainly on logos to detect and recognize its target brand. Given the rapid changes in webpage visuals, including various screenshots in the target list is challenging. The strength of these two models is they are not sensitive to brand changes. When testing on datasets with unknown brands without logo datasets, they would work well.

**Takeaway 5:** Logo-based methods are effective in phishing detection and brand identification but vulnerable to novel logo variations. Screenshot-based methods are more stable across brands but struggle with web design diversity. **PhishZoo**'s performance suggests issues with keyword selection. Careful feature selection is crucial, and all methods have potential weaknesses.

### 5.3 Case Study of Detection Failures

We conducted a manual investigation into 500 samples that failed to be detected, randomly selected from the dataset, to determine the underlying reasons for the detection failures. Particularly, **PhishIntention** and **Phishpedia** generally demonstrate good performance in phishing detection and brand identification tasks. However, their effectiveness can be inconsistent when encountering changed captions. For example, as shown in Figure 5-(f), **PhishIntention** successfully detects it as a phishing webpage targeted to Facebook with a 0.95 similarity score to the brand reference list, while **Phishpedia** fails in the detection because its similarity score fell below the threshold. This discrepancy can be attributed to the

OCR-aided Siamese model used by **PhishIntention**, which incorporates additional textual information for the logo. Although **EMD** successfully detects the phishing attack with a distance of 0.93, it does not recognize the targeted brand. **Involution**, **PhishZoo** and **VisualPhiNet** can find the candidate and identify the target brand with a similarity of 0.85, 60.92, and 0.82, respectively. Therefore, **Phishpedia** is vulnerable to the caption change.

One reason that causes **PhishZoo** to have high performance in phishing detection but fails in identification is that it selects the wrong candidate. For example, Figure 5-(e) shows the Scaling influence. It selects 'arrow menu,' 'the,' 'your,' 'at,' and 'verse' as the keywords from benign target HTML, while 'yahoo,' 'PHP,' 'login,' 'same attendance,' 'screen' and 'index.' Both of them do not include the actual keyword, which decreases the performance. In this scenario, only **VisualPhishNet** can not find the target brand.

For the screenshots without a logo, the **PhishIntention**, **Phishpedia**, and **Involution** fail in detection. For example, Figure 5-(b) will not be detected by these models but can be detected by **PhishZoo** with the other brand. For **VisualPhishNet**, although it mispredicts as benign, it can recognize the target brand with a similarity 1.11. Based on the evaluation results, we further find more failure examples in the APWG evaluation dataset for different models. Detailed examples can refer to Appendix A.3.

## 6 MANIPULATED VISUAL COMPONENTS

We observe that in our dataset, phishing attackers employ a new tactic where they manipulate visual components to bypass visual similarity-based anti-phishing models, which motivates us to evaluate the robustness of the models against the manipulations.

**Evaluation Plan.** The manipulated samples are equipped with original benign URLs and HTML for evaluation by default. As **PhishIntention** and **Phishpedia** use domains to identify the brand, we also test the influence of squatted domains (e.g., `faceb00k.com`) by using crafted visual images with 'typosquatting' domains to replace the original benign URLs. Note that for these two methods, the numbers in the row of 'Original' in the table (Table 4 and Table 5) and with benign URLs mean *misclassified*, while for other methods, it means the number is correctly *classified*. These numbers are the upper bound for not being equipped with domain check methods. The detection and brand identification results are shown in Table 4 and Table 5, respectively.

**Reference Target List.** The logo-based and screenshot-based models use the extended logo and screenshot brand target lists, respectively. We also utilize the maintained domain list provided by **PhishIntention**.

**Evaluation Metric.** For testing benign samples, let the number of benign samples as  $N_n$ , the number of benign samples reported as benign be  $N_{tn}$ , and the number of correctly identifying the target brand for benign as  $I_{tn}$ . The detection accuracy is  $I_{tn}/N_n$ , identification rate is  $I_{tn}/N_{tn}$ , identification rate out of total is  $I_{tn}/N_n$ . For phishing samples, the metric is the same as in Section 5.

### 6.1 Robustness Evaluation

**Legitimate Logo and URL (False Positive).** Taking phishing as positive, when testing models with benign samples (legitimate logos and URLs), they are expected to correctly identify them as legitimate websites since URLs like 'facebook.com' are genuine and

**Table 4: Evaluation Result of Phishing Detection with Manipulated Visual Components (i.e., Classified as Phishing). Models, trained on  $D_{tr2}$ , are used for evaluation. The row means manipulating type, the original is the brands' recent benign webpage, visible manipulation and perturbation-based manipulation refer to the dataset crafted for robustness testing. The column for different models means URL type, benign refers to the original benign URL while squatted means the created URLs. Default benign URLs are used.**

Manipulation ID	PhishIntention		Phishpedia		Involution	PhishZoo	VisualPhishNet	EMD
	Benign	Squatted	Benign	Squatted				
Original	3/110 (2.73%)	316/1,321 (23.92%)	7/110 (6.36%)	894/1,321 (67.68%)	88/110 (80.00%)	108/110 (98.18%)	30/110 (27.27%)	55/110 (50.00%)
Visible Manipulation	1. Deletion	0/110 (0.0%)	10/1,321 (0.76%)	10/110 (9.09%)	151/1,321 (11.43%)	3/110 (2.73%)	103/110 (93.64%)	28/110 (25.45%)
	2. Color	4/580 (0.69%)	858/6,925 (12.32%)	44/580 (7.59%)	1,248/6,925 (17.92%)	327/580 (56.38%)	562/580 (96.90%)	125/580 (21.55%)
	3. Ratio	29/877 (3.30%)	2,230/10,532 (21.17%)	65/877 (7.41%)	6,383/10,532 (60.61%)	696/877 (79.36%)	856/877 (97.61%)	242/877 (27.59%)
	4. Rotation	36/1,320 (2.73%)	3,612/15,852 (22.79%)	96/1,320 (7.27%)	10,442/15,852 (65.87%)	1,085/1,320 (82.20%)	1,283/1,320 (97.20%)	387/1,320 (29.32%)
	5. Combination	22/369 (5.96%)	817/4,431 (18.44%)	58/369 (15.72%)	2,624/4,431 (59.22%)	217/369 (58.81%)	362/369 (98.10%)	95/369 (25.75%)
	6. Location	24/879 (2.73%)	2,035/10,556 (19.28%)	66/879 (7.51%)	6,278/10,556 (59.47%)	587/879 (66.78%)	870/879 (98.98%)	216/879 (24.57%)
	7. Flipping	4/220 (1.82%)	459/2,642 (17.37%)	16/220 (7.27%)	1,692/2,642 (64.04%)	28/220 (12.73%)	216/220 (98.18%)	62/220 (28.18%)
	8. Replacement	177/1,006 (17.59%)	2,202/12,081 (18.23%)	444/1,006 (44.14%)	5,545/12,081 (45.90%)	502/1,006 (49.90%)	967/1,006 (96.12%)	235/1,006 (23.36%)
	9. Blurring	1/110 (0.91%)	122/1,321 (9.24%)	3/110 (2.73%)	426/1,321 (32.20%)	32/110 (29.09%)	102/110 (92.73%)	29/110 (26.36%)
	10. Scaling	20/550 (3.64%)	1,530/6,605 (23.16%)	41/550 (7.45%)	4,536/6,605 (68.68%)	461/550 (83.82%)	538/550 (97.82%)	147/550 (26.73%)
	11. Division	2/96 (2.08%)	114/1,152 (9.90%)	11/96 (11.46%)	451/1,152 (39.15%)	52/96 (54.17%)	93/96 (96.88%)	34/96 (35.42%)
	12. Font	4/186 (2.15%)	294/2,232 (13.17%)	23/186 (12.37%)	774/2,232 (34.68%)	115/186 (61.83%)	179/186 (96.24%)	56/186 (30.11%)
	13. Case	6/225 (2.67%)	299/2,700 (11.07%)	36/225 (16.00%)	960/2,700 (35.56%)	76/225 (33.78%)	214/225 (95.11%)	73/225 (32.44%)
Total		329/6,528 (5.04%)	14,582/78,390 (18.60%)	913/6,528 (13.99%)	41,510/78,390 (52.95%)	4,181/6,528 (64.05%)	6,345/6,528 (97.20%)	1,729/6,528 (26.49%)
Perturbation-based	SRNet	11/41 (26.83%)	114/492 (23.17%)	34/41 (82.93%)	347/492 (70.53%)	25/41 (60.98%)	39/41 (95.12%)	11/41 (26.83%)
	[22]-ViT	3/110 (2.73%)	266/1,321 (20.14%)	8/110 (7.27%)	696/1,321 (52.69%)	82/110 (74.55%)	106/110 (96.36%)	34/110 (30.91%)
	[22]-Swin	3/110 (2.73%)	296/1,321 (22.41%)	10/110 (9.09%)	820/1,321 (62.07%)	86/110 (78.18%)	108/110 (98.18%)	34/110 (30.91%)
	FGSM	4/110 (3.64%)	279/1,321 (21.12%)	8/110 (7.27%)	776/1,321 (58.74%)	80/110 (72.73%)	106/110 (96.36%)	30/110 (27.27%)
	PGD	4/110 (3.64%)	259/1,321 (19.61%)	8/110 (7.27%)	756/1,321 (57.23%)	79/110 (71.82%)	106/110 (96.36%)	30/110 (27.27%)
	CW	4/110 (3.64%)	269/1,321 (20.36%)	10/110 (9.09%)	790/1,321 (59.80%)	80/110 (72.73%)	106/110 (96.36%)	30/110 (27.27%)
Total		18/550 (3.27%)	1,369/6,605 (20.71%)	44/550 (8.00%)	3,838/6,605 (58.11%)	407/550 (74.00%)	532/550 (96.72%)	158/550 (28.73%)
262/550 (47.64%)								

not indicative of phishing. If a model incorrectly flags such benign samples as potential phishing attempts, it results in a false positive error, labeling legitimate websites as phishing threats.

We begin by evaluating how often the models incorrectly flag legitimate websites as potential phishing threats (the false positive rate). Specifically, **PhishIntention** detects three benign samples (with legitimate domains) as phishing, whereas **Phishpedia** identifies seven benign samples as phishing. The misclassification stems from the model's reliance on a domain list to verify the legitimacy of the logos. Some legitimate domains, such as 'santanderbank', are not included in the list, although 'santander' and 'santander-research' exist in the list. This oversight highlights the limitations of relying on incomplete reference lists for verification purposes.

**Takeaway 6:** Models that rely on incomplete reference lists for verifying the legitimacy of logos and domains are prone to false positive errors, incorrectly flagging legitimate websites as phishing threats.

**Visible and Perturbation-based Manipulation Methods.** In our evaluation of **PhishZoo** on visible manipulation and perturbation-based adversarial manipulation datasets, we observe that while different strategies impact the identification result, they do not affect the detection result very significantly. Specifically, it achieves a 97.20% detection rate on the perturbation-based adversarial manipulation dataset and 96.72% on the visible manipulation dataset. In the perturbation-based scenarios, removing the logo, blurring, changing font manually or by **SRNet**, and converting cases are critical factors in the model's phishing detection capability. Except for the former factors, replacing logos markedly influences identification results, though **PhishZoo** is less sensitive to the use of

combined logos. Additionally, **PhishZoo** is sensitive to the white-box attack in phishing identification, which means it is not robust on the perturbated manipulation dataset.

For other logo-based approaches, manipulations such as logo deletion, flipping, blurring, and case conversion substantially affect detection results. Meanwhile, changing colors, combining logos, or replaced with other logos play important roles in identification. Although logo text font greatly affects **Phishpedia**, it does not significantly impact **Involution**.

Visible manipulations are more easily detected by these models than perturbation-based adversarial ones, but they are challenging for people to notice. Although perturbation-based manipulation attack influence is not as great as the visible manipulation, they reveal vulnerabilities in the models: **PhishIntenion** and **Phishpedia** are sensitive to the ViT-based black box attack and the PGD white box attack. **Involution** is not robust on white box attacks, and **PhishZoo** is vulnerable to both attacks. For screenshot-based methods, detection performance remains stable across various manipulations, with perturbation-based manipulation strategies even improving detection rates in **VisualPhishNet**. However, these methods struggle with accurately identifying the target brand. Additionally, decreased performance observed when logos are deleted, replaced, or divided in identification results underscores the crucial role of logos in brand recognition within screenshot-based methods.

**Takeaway 7:** Phishing detection models can be vulnerable to various logo manipulation techniques. Visible manipulations significantly impact logo-based methods, while perturbated manipulations reveal weaknesses in the models. Screenshot-based methods maintain stable detection but struggle with brand identification when logos are altered.

**Table 5: Evaluation Result of Phishing Brand Identification with Manipulated Visual Component.** Models, trained on  $D_{tr2}$ , are used for evaluation. The row means manipulating type, the original is the brands' recent benign webpage, visible manipulation and perturbation-based adversarial manipulation refer to the dataset crafted for robustness testing. The column for models means URL type, benign means original benign URL, while squatted means the created URLs. The percentage is the correctly identified brands out of the predicted phishing number.

Manipulation ID	PhishIntention		Phishpedia		Involution	PhishZoo	VisualPhishNet	EMD	
	Benign	Squatted	Benign	Squatted					
Original	3/3 (100.0%)	316/316 (100.0%)	6/7 (85.71%)	882/894 (98.66%)	87/88 (98.86%)	35/108 (32.41%)	16/30 (53.33%)	11/55 (20.0%)	
Visible Manipulation	1. Deletion	0/0 (0.0%)	10/10 (100.0%)	0/10 (0.0%)	30/151 (19.87%)	3/3 (100.0%)	7/103 (6.80%)	6/28 (25.43%)	9/54 (16.67%)
	2. Color	4/4 (100.0%)	858/858 (100.0%)	6/44 (13.64%)	792/1,248 (63.46%)	322/327 (98.47%)	69/562 (12.28%)	39/125 (31.20%)	49/275 (17.82%)
	3. Ratio	29/29 (100.0%)	2,230/2,230 (100.0%)	42/65 (64.62%)	6,112/6,383 (95.75%)	688/696 (98.85%)	160/856 (18.69%)	140/242 (57.85%)	80/421 (19.00%)
	4. Rotation	36/36 (100.0%)	3,612/3,612 (100.0%)	81/96 (84.38%)	10,262/10,442 (98.28%)	1,072/1,085 (98.80%)	389/1,283 (30.32%)	202/387 (52.20%)	121/671 (18.03%)
	5. Combination	9/22 (40.91%)	661/817 (80.91%)	23/58 (39.66%)	2,206/2,624 (84.07%)	188/217 (86.64%)	119/362 (32.87%)	38/95 (40.00%)	37/188 (19.68%)
	6. Location	24/24 (100.0%)	2,035/2,035 (100.0%)	47/66 (71.21%)	6,051/6,278 (96.38%)	578/587 (98.47%)	288/870 (33.10%)	103/216 (47.69%)	79/432 (18.29%)
	7. Flipping	4/4 (100.0%)	459/459 (100.0%)	13/16 (81.25%)	1,656/1,692 (97.87%)	28/28 (100.0%)	28/216 (12.96%)	34/62 (54.84%)	19/107 (17.76%)
	8. Replacement	0/177 (0.0%)	70/2,202 (3.18%)	0/444 (0.0%)	210/5,545 (3.79%)	27/502 (5.38%)	63/967 (6.51%)	63/235 (26.81%)	67/468 (14.32%)
	9. Blurring	1/1 (100.0%)	122/122 (100.0%)	1/3 (33.33%)	402/426 (94.37%)	23/32 (71.88%)	5/102 (4.90%)	17/29 (58.62%)	11/51 (21.57%)
	10. Scaling	20/20 (100.0%)	1,530/1,530 (100.0%)	35/41 (85.37%)	4,466/4,536 (98.46%)	455/461 (98.70%)	155/538 (28.81%)	89/147 (60.54%)	48/274 (17.52%)
	11. Division	2/2 (100.0%)	114/114 (100.0%)	3/11 (27.27%)	355/451 (78.71%)	47/52 (90.38%)	20/93 (21.51%)	8/34 (23.53%)	5/42 (11.90%)
	12. Font	4/4 (100.0%)	294/294 (100.0%)	5/23 (21.74%)	558/774 (72.09%)	111/115 (96.52%)	24/179 (13.41%)	25/56 (44.64%)	17/90 (18.89%)
	13. Case	3/6 (50.0%)	263/299 (87.96%)	5/36 (13.89%)	588/960 (61.25%)	74/76 (97.37%)	25/214 (11.68%)	36/73 (49.32%)	20/113 (17.70%)
Total		136/329 (41.34%)	12,258/14,582 (84.06%)	261/913 (28.59%)	33,688/41,510 (81.16%)	3,616/4,181 (86.49%)	1,352/6,345 (21.31%)	800/1,729 (46.27%)	562/3,186 (17.64%)
SRNET		11/11 (100.0%)	114/114 (100.0%)	34/34 (100.0%)	347/347 (100.0%)	25/25 (100.0%)	6/39 (15.38%)	5/11 (45.45%)	3/20 (15.00%)
Perturbation-based	[22]-ViT	3/3 (100.0%)	266/266 (100.0%)	4/8 (50.00%)	648/696 (93.10%)	81/82 (98.78%)	27/106 (25.47%)	18/34 (52.94%)	10/52 (19.23%)
	[22]-Swin	3/3 (100.0%)	296/296 (100.0%)	6/10 (60.00%)	772/820 (94.15%)	85/86 (98.84%)	35/108 (32.41%)	17/34 (50.00%)	12/55 (21.82%)
	FSGM	4/4 (100.0%)	279/279 (100.0%)	6/8 (75.00%)	752/776 (96.91%)	79/80 (98.75%)	19/106 (17.92%)	15/30 (50.00%)	9/52 (17.31%)
	PGD	4/4 (100.0%)	259/259 (100.0%)	6/8 (75.00%)	732/756 (96.83%)	78/79 (98.73%)	14/106 (13.21%)	14/30 (46.67%)	7/51 (13.73%)
	CW	4/4 (100.0%)	269/269 (100.0%)	6/10 (60.00%)	742/790 (93.92%)	79/80 (98.75%)	19/106 (17.92%)	15/30 (50.00%)	9/52 (17.31%)
Total		18/18 (100.0%)	1,369/1,369 (100.0%)	28/44 (63.64%)	3,646/3,838 (95.00%)	236/239 (98.74%)	114/532 (21.43%)	79/158 (50.00%)	47/262 (17.94%)

**Benign Vs. Squatted Domains.** When comparing benign and squatted URLs, we observe that the domain is essential to PhishIntention and Phishpedia. The structure of these two models detects the target brand of screenshots and compares the detected brand's domain with the parsed URL domain. Therefore, testing with benign URLs or squatted will highly influence the detection results. If the testing samples have a high similarity or directly use benign logos with the same domain, they will think they are benign if the similarity is higher than the threshold. It also means that if the attackers can successfully manage the URL parsing with the same domain, they can pass the detection model even if they directly use benign logos. When testing, we found that the squatting successfully passed the model when producing the same domain as the benign one, like 'www.capitalone.aaa,' which targets the 'www.capitalone.com.' Furthermore, we find how parsing the URL plays an integral part in the detection methods. For example, the `tldextract` [47] will parse the 'https://home.barclays/' domain to 'home' rather than the 'barclays.'

**Takeaway 8:** Models rely on domain checking heavily depending on how the URL is parsed and compared against the maintained second-level domain.

## 6.2 Case Study of Failures

We find that texts in the visual components play an important role in phishing detection and phishing brand identification. PhishIntention incorporates the OCR part to help the model learn more textual information compared to Phishpedia. For example, when testing the original screenshot of 'Rackspace' (American cloud computing company) with the benign URL, PhishIntention can



Figure 3: Text Influence Case (Original logo and benign URL).

identify the brand while Phishpedia predicts it as 'timeweb,' as shown in Figure 3.

Table 2 displays the cropped logos obtained from the produced screenshots based on 'Youtube' for each manipulation. We assess the similarity of these logos of crafted screenshots against brand reference lists. We find that the manipulations 'Deletion,' 'Color,' and 'Combination' achieve the similarity scores of 0.6, 0.5, and 0.6 for Phishpedia. Other manipulations are around 0.9. Since the HTML does not contain CRP, PhishIntention will consider all of them to be benign. PhishZoo identifies the appropriate candidate keywords in this example, with similarity scores of 66.3, 67.5, 57.8, 65.1, 53.0, 47.0 for 'Rotation,' 'Combination,' 'Ratio,' 'Scaling,' 'Color,' and 'Flipping' manipulation. After cropping the logo from screenshots by Faster RCNN, Involution fails to recognize the brand and the similarities are around 0.57 except the 'Case' example which is recognized as 'AOL.' All examples in VisualPhishNet are around 1.1 to 1.3 and misclassified as other brands, like 'alibaba,' EMD distance is 0.96 and predicted as 'Airbnb.'

**Takeaway 9:** Visible manipulations of logos can significantly impact the accuracy of phishing detection systems, highlighting the need for more robust approaches that incorporate both textual and visual information.

## 7 DISCUSSION

**Recommendations.** We suggest recommendations to develop more comprehensive and resilient visual similarity-based phishing detection systems against visual component manipulation attacks. We recommend integrating text recognition techniques to robustly defend against textual manipulations like caption changes. Leveraging OCR-aided deep learning models can enhance brand identification on the image and can also help candidate selection for phishing detection. This approach addresses the limitations observed in methods such as Phishpedia, which may not effectively account for semantic variations in phishing attempts.

It is crucial to incorporate adversarial examples and manipulated logos in the training data through data augmentation techniques. By exposing models to various real-world logo manipulation patterns, such as scaling, rotation, and color changes, the systems can enhance their ability to withstand adversarial attacks and proactively recognize subtle visual manipulations. To improve detection robustness and mitigate targeted attacks on specific components, we advise adopting a multi-cue ensemble approach that amalgamates the analysis of logos, webpage layouts, textual content, and other visual elements.

Moreover, we recommend employing preprocessing and normalization techniques, including image scaling and denoising, prior to visual similarity analysis. These methods can reduce the efficacy of adversarial manipulations and provide an additional layer of defense against sophisticated phishing tactics.

**Limitations.** Our work has a few key limitations. First, the lack of a user study limits the assessment of our manipulation methods' effectiveness in real-world scenarios, as users may readily recognize manipulated logo images. To address this, we perform manual verification with 500 randomly generated images to ensure our manipulations are not easily recognizable. However, a comprehensive user study would be valuable for gathering insights into the perceptibility and deceptiveness of adversarial manipulations. Second, our analysis is limited to logo manipulations and does not consider other visual components or webpage elements that could be targeted. Expanding the scope could provide a more comprehensive understanding of potential attack vectors. Third, our evaluation is conducted only on models and datasets with publicly available source code and data. Despite these limitations, we highlight the potential vulnerabilities of visual similarity-based anti-phishing systems and the need for robust defense mechanisms against adversarial visual manipulations.

## 8 RELATED WORK

**Evaluation of Visual Similarity-based Phishing Detection.** Visual similarity-based phishing detection systems compare the visual features of suspicious websites with known benign ones to identify phishing attempts. Unfortunately, comprehensive evaluations of their real-world effectiveness are limited. Prior work primarily used datasets and was tested in controlled environments, which may only partially reflect real-world challenges. Panum *et al.* [48] analyzed the robustness of phishing detectors to perturbation attacks, while Abuadba *et al.* [49] identified web phishing trends that bypass traditional machine learning-based detectors and proposed a

logistic regression-based model for detection. However, their evaluations were limited in scope. Zieni *et al.* [50] and Hou *et al.* [51] provided literature reviews on phishing website detection and logo detection techniques, respectively, but did not conduct comparative analyses or provide direct results across different methods. Miao *et al.* [52] evaluated Google's phishing detectors but did not extend their study to other deep learning-based systems.

To the best of our knowledge, our work is the first to comprehensively evaluate various visual similarity-based phishing detection models under the same, controlled environment (the same large-scale, real-world dataset). While Liu *et al.* [4] introduced the PhishIntention model and evaluated it against several baselines, our analysis goes further by assessing the performance of detectors on a substantial dataset of real phishing websites sourced from APWG. We also comprehensively compare the performance of the models at both the macroscopic and granular levels, providing valuable insights into their effectiveness and robustness in the real world.

**Evaluation of Robustness against Adversarial Manipulation.** Adversarial attacks against machine learning models leverage designed perturbations to the input data, referred to as adversarial samples, to elicit model predictions that align with the attacker's objectives [41, 42]. These perturbations, often imperceptible to the human eye, can deceive even the most sophisticated ML models. In the context of phishing attacks, adversaries must ensure that manipulated visual components not only effectively deceive potential victims but also bypass phishing defense systems. Lee *et al.* [22] introduced an adversarial learning-based framework that applies perturbation vectors to target logos, enabling them to bypass phishing detectors while remaining undetectable to human eyes. Despite the potential threat of adversarial attacks, prior research has not thoroughly investigated the robustness of phishing detection models against various manipulation attacks. Our study aims to address this gap by examining the weaknesses of these models against various manipulation techniques, including 14 types of visible manipulations and 5 adversarial perturbations. Interestingly, our findings suggest bypass is more likely when a slight visible manipulation is applied than perturbation-based manipulations.

## 9 CONCLUSION

We conduct the first comprehensive evaluation of state-of-the-art visual similarity models for phishing detection using a large-scale dataset of 450K real-world phishing websites, involving six visual similarity-based anti-phishing models. Our analysis reveals significant gaps between model performance in real-world scenarios and their reported results on curated datasets, highlighting the importance of evaluations with real-world datasets. We identify specific weaknesses of each model that phishers could exploit through adversarial visual manipulations, necessitating more robust defense mechanisms. To enhance robustness against textual manipulations, we recommend integrating text recognition techniques with visual analysis. Crucially, data augmentation incorporating adversarial examples and real-world manipulation patterns is essential for improving models' resilience to adversarial attacks. We advise adopting a multi-cue ensemble approach to mitigate targeted attacks on specific components. Additionally, employing preprocessing techniques like scaling and denoising can further reduce the impact of adversarial perturbations.

## REFERENCES

[1] Suzanne Widup, Alex Pinto, David Hylander, Gabriel Bassett, and Philippe lan-glois. Verizon Data Breach Investigations Report, 2021.

[2] Grant Ho, Asaf Cidon, Lior Gavish, Marco Schweighauser, Vern Paxson, Stefan Savage, Geoffrey M Voelker, and David Wagner. Detecting and characterizing lateral phishing at scale. In *Proc. of the USENIX Security Symposium*, 2019.

[3] Yun Lin, Ruofan Liu, Dinil Mon Divakaran, Jun Yang Ng, Qing Zhou Chan, Yiwen Lu, Yuxuan Si, Fan Zhang, and Jin Song Dong. Phishpedia: A hybrid deep learning based approach to visually identify phishing webpages. In *Proc. of the USENIX Security Symposium*, 2021.

[4] Ruofan Liu, Yun Lin, Xianglin Yang, Siang Hwee Ng, Dinil Mon Divakaran, and Jin Song Dong. Inferring phishing intention via webpage appearance and dynamics: A deep vision based approach. In *Proc. of the USENIX Security Symposium*, 2022.

[5] Sahar Abdelnabi, Katharina Krombholz, and Mario Fritz. Visualphishnet: Zero-day phishing website detection by visual similarity. In *Proc. of the 2020 ACM SIGSAC Conference on Computer and Communications Security*, 2020.

[6] Anthony Y. Fu, Liu Wenying, and Xiaotie Deng. Detecting phishing web pages with visual similarity assessment based on earth mover's distance (emd). *IEEE Transactions on Dependable and Secure Computing*, 2006.

[7] Wenying Liu, Xiaotie Deng, Guanglin Huang, and Anthony Y Fu. An antiphishing strategy based on visual similarity assessment. *IEEE Internet Computing*, 2006.

[8] Sadia Afroz and Rachel Greenstadt. Phishzoo: Detecting phishing websites by looking at them. In *Proc. of the 2011 IEEE Fifth International Conference on Semantic Computing*, 2011.

[9] Karen Sparck Jones. A statistical interpretation of term specificity and its application in retrieval. *Journal of documentation*, 1972.

[10] Safe Browsing – Google Safe Browsing. (Accessed on 10/30/2023). URL: <https://safebrowsing.google.com/>.

[11] Adam Oest, Penghui Zhang, Brad Wardman, Eric Nunes, Jakub Burgis, Ali Zand, Kurt Thomas, Adam Doupé, and Gail-Joon Ahn. Sunrise to sunset: Analyzing the end-to-end life cycle and effectiveness of phishing attacks at scale. In *Proc. of the USENIX Security Symposium*, 2020.

[12] Hyunsang Choi, Bin B. Zhu, and Heejoo Lee. Detecting malicious web links and identifying their attack types. In *Proc. of the USENIX Conference on Web Application Development*, 2011.

[13] Mohammed Nazin Feroz and Susan Mengel. Phishing url detection using url ranking. In *IEEE International Congress on Big Data*, 2015.

[14] Hung Le, Quang Pham, Doyen Sahoo, and Steven C. H. Hoi. Urlnet: Learning a URL representation with deep learning for malicious URL detection. *arXiv preprint arXiv:1802.03162*, 2018.

[15] Jonathan Woodbridge, Hyrum S. Anderson, Anjum Ahuja, and Daniel Grant. Detecting homoglyph attacks with a siamese neural network. In *Proc. of the IEEE Security and Privacy Workshops*, 2018.

[16] Shuaiji Li, Tao Huang, Zhiwei Qin, Fanfang Zhang, and Yinhong Chang. Domain generation algorithms detection through deep neural network and ensemble. In *Proc. of the ACM Web Conference*, 2019.

[17] Manuel Sánchez-Paniagua, Eduardo Fidalgo Fernández, Enrique Alegre, We-sam Al-Nabki, and Victor González-Castro. Phishing url detection: A real-case scenario through login urls. *IEEE Access*, 2022.

[18] Frank L Hitchcock. The distribution of a product from several sources to numerous localities. *Journal of mathematics and physics*, 1941.

[19] Wenying Liu, Xiaotie Deng, Guanglin Huang, and Anthony Y Fu. An antiphishing strategy based on visual similarity assessment. *IEEE Internet Computing*, 2006.

[20] Shaqiq Ren, Kaiming He, Ross B. Girshick, and Jian Sun. Faster R-CNN: towards real-time object detection with region proposal networks. In *Proc. of the Advances in Neural Information Processing Systems*, 2015.

[21] Duo Li, Jie Hu, Changhu Wang, Xiangtai Li, Qi She, Lei Zhu, Tong Zhang, and Qifeng Chen. Involution: Inverting the inherence of convolution for visual recognition. In *Proc. of the IEEE/CVF Conference on Computer Vision and Pattern Recognition*, 2021.

[22] Jehyun Lee, Zhe Xin, Melanie Ng Pei See, Kanav Sabharwal, Giovanni Apruzzese, and Dinil Mon Divakaran. Attacking logo-based phishing website detectors with adversarial perturbations. *arXiv preprint arXiv:2308.09392*, 2023.

[23] The APWG eCrime Exchange (eCX). (Accessed on 04/22/2024). URL: <https://apwg.org/ecx/>.

[24] The Selenium Browser Automation Project. (Accessed on 04/12/2024). URL: <https://www.selenium.dev/documentation/>.

[25] Babak Amin Azad, Oleksii Starov, Pierre Laperdrix, and Nick Nikiforakis. Web runner 2049: Evaluating third-party anti-bot services. In *Proc. of the Detection of Intrusions and Malware, and Vulnerability Assessment*, 2020.

[26] Xigao Li, Babak Amin Azad, Amir Rahmati, and Nick Nikiforakis. Good bot, bad bot: Characterizing automated browsing activity. In *Proc. of the IEEE Symposium on Security and Privacy*, 2021.

[27] Adam Oest, Yeganeh Safaei, Penghui Zhang, Brad Wardman, Kevin Tyers, Yan Shoshitaishvili, and Adam Doupé. PhishTime: Continuous longitudinal measurement of the effectiveness of anti-phishing blacklists. In *Proc. of the USENIX Security Symposium*, 2020.

[28] Adam Oest, Yeganeh Safaei, Adam Doupé, Gail-Joon Ahn, Brad Wardman, and Kevin Tyers. Phishfarm: A scalable framework for measuring the effectiveness of evasion techniques against browser phishing blacklists. In *Proc. of the IEEE Symposium on Security and Privacy*, 2019.

[29] Doowon Kim, Haehyun Cho, Yonghwi Kwon, Adam Doupé, Sooel Son, Gail-Joon Ahn, and Tudor Dumitras. Security analysis on practices of certificate authorities in the https phishing ecosystem. In *Proc. of the ACM Asia Conference on Computer and Communications Security*, 2021.

[30] Penghui Zhang, Adam Oest, Haehyun Cho, Zhibo Sun, RC Johnson, Brad Wardman, Shaown Sarker, Alexandros Kapravelos, Tiffany Bao, Ruoyu Wang, Yan Shoshitaishvili, Adam Doupé, and Gail-Joon Ahn. Crawlpish: Large-scale analysis of client-side cloaking techniques in phishing. In *Proc. of the IEEE Symposium on Security and Privacy*, 2021.

[31] Adam Oest, Yeganeh Safaei, Adam Doupé, Gail-Joon Ahn, Brad Wardman, and Gary Warner. Inside a phisher's mind: Understanding the anti-phishing ecosystem through phishing kit analysis. In *Proc. of the APWG Symposium on Electronic Crime Research*, 2018.

[32] Fastdup. GitHub - visual-layer/fastdup. (Accessed on 04/24/2024). URL: <https://github.com/visual-layer/fastdup>.

[33] Ostap Viniavskyi, Mariia Dobko, Dmytro Mishkin, and Oles Dobosevych. Openglue: Open source graph neural net based pipeline for image matching. *arXiv preprint arXiv:2204.08870*, 2022.

[34] WhatTheFont Font Finder - Identify Fonts by Image. (Accessed on 04/24/2024). URL: <https://www.myfonts.com/pages/whatthefont>.

[35] Liang Wu, Chengquan Zhang, Jiaming Liu, Junyu Han, Jingtuo Liu, Errui Ding, and Xiang Bai. Editing text in the wild. In *Proc. of the 27th ACM International Conference on Multimedia*, 2019.

[36] Zhanghan Ke, Yuhao Liu, Lei Zhu, Nanxuan Zhao, and Rynson W. H. Lau. Neural preset for color style transfer. *arXiv preprint arXiv:2303.13511*, 2023.

[37] Qiangpeng Yang, Hongsheng Jin, Jun Huang, and Wei Lin. Swaptext: Image based texts transfer in scenes. *arXiv preprint arXiv:2003.08152*, 2020.

[38] Karthika Subramani, William Melicher, Oleksii Starov, Phani Vadrevu, and Roberto Perdisci. Phishinpatterns: Measuring elicited user interactions at scale on phishing websites. In *Proc. of the ACM Internet Measurement Conference*, 2022.

[39] Remove Background from Image for Free – remove.bg. (Accessed on 03/15/2024). URL: <https://www.remove.bg/>.

[40] Christian Szegedy, Wojciech Zaremba, Ilya Sutskever, Joan Bruna, Dumitru Erhan, Ian Goodfellow, and Rob Fergus. Intriguing properties of neural networks. *arXiv preprint arXiv:1312.6199*, 2013.

[41] Ian J. Goodfellow, Jonathon Shlens, and Christian Szegedy. Explaining and harnessing adversarial examples. In *Proc. of the International Conference on Learning Representations*, 2015.

[42] Aleksander Madry, Aleksandar Makelov, Ludwig Schmidt, Dimitris Tsipras, and Adrian Vladu. Towards deep learning models resistant to adversarial attacks. In *Proc. of the International Conference on Learning Representations*, 2018.

[43] N. Carlini and D. Wagner. Towards evaluating the robustness of neural networks. In *Proc. of the IEEE Symposium on Security and Privacy*, 2017.

[44] Alexey Dosovitskiy, Lucas Beyer, Alexander Kolesnikov, Dirk Weissenborn, Xiaohua Zhai, Thomas Unterthiner, Mostafa Dehghani, Matthias Minderer, Georg Heigold, Sylvain Gelly, Jakob Uszkoreit, and Neil Houlsby. An image is worth 16x16 words: Transformers for image recognition at scale. *arXiv preprint arXiv:2010.11929*, 2021.

[45] Ze Liu, Yutong Lin, Yue Cao, Han Hu, Yixuan Wei, Zheng Zhang, Stephen Lin, and Baining Guo. Swin transformer: Hierarchical vision transformer using shifted windows. *arXiv preprint arXiv:2103.14030*, 2021.

[46] GitHub - typosquatter/ail-typo-squatting: Generate list of potential typo squatting domains with domain name permutation engine to feed AIL and other systems. (Accessed on 04/08/2024). URL: <https://github.com/typosquatter/ail-typo-squatting>.

[47] Github - john-kurkowski/tldextract: Accurately separates a url's subdomain, domain, and public suffix, using the public suffix list (psl). (Accessed on 04/30/2024). URL: <https://github.com/john-kurkowski/tldextract>.

[48] Thomas Kobber Panum, Kaspar Hageman, René Rydhof Hansen, and Jens Myrup Pedersen. Towards adversarial phishing detection. In *Proc. of the USENIX Workshop on Cyber Security Experimentation and Test*, 2020.

[49] Alsharif Abuadba, Shuo Wang, Mahathir Almarshi, Mohammed Ejaz Ahmed, Raj Gaire, Seyit Camtepe, and Surya Nepal. Towards Web Phishing Detection Limitations and Mitigation, 2022.

[50] Rasha Zieni, Luisa Massari, and Maria Carla Calzarossa. Phishing or not phishing? a survey on the detection of phishing websites. *IEEE Access*, 2023.

[51] Sujuan Hou, Jiacheng Li, Weiqing Min, Qiang Hou, Yanna Zhao, Yuanjie Zheng, and Shuqiang Jiang. Deep learning for logo detection: A survey. *ACM Trans. Multimedia Comput. Commun. Appl.*, 2023.

[52] Changqing Miao, Jianan Feng, Wei You, Wenchang Shi, Jianjun Huang, and Bin Liang. A good fishman knows all the angles: A critical evaluation of google's phishing page classifier. In *Proc. of the 2023 ACM SIGSAC Conference on Computer and Communications Security*, 2023.

[53] Liu Wenyin, Guanglin Huang, Liu Xiaoyue, Zhang Min, and Xiaotie Deng. Detection of phishing webpages based on visual similarity. In *Proc. of the Special Interest Tracks and Posters of the International Conference on World Wide Web*, 2005.

[54] Eric Medvet, Engin Kirda, and Christopher Kruegel. Visual-similarity-based phishing detection. In *Proc. of the ACM International Conference on Security and Privacy in Communication Networks*, 2008.

[55] Kuan-Ta Chen, Jau-Yuan Chen, Chun-Rong Huang, and Chu-Song Chen. Fighting phishing with discriminative keypoint features. *IEEE Internet Computing*, 2009.

[56] Matthew Dunlop, Stephen Groat, and David Shelly. Goldphish: Using images for content-based phishing analysis. In *Proc. of the IEEE International Conference on Internet Monitoring and Protection*, 2010.

[57] Marisa Bernabeu, Antonio Javier Gallego, and Antonio Pertusa. Multi-label logo recognition and retrieval based on weighted fusion of neural features. *arXiv preprint arXiv:2205.05419*, 2022.

[58] Muhammet Bastan, Hao-Yu Wu, Tian Cao, Bhargava Kota, and Mehmet Tek. Large scale open-set deep logo detection. *arXiv preprint arXiv:1911.07440*, 2019.

[59] Manish Bhurtel, Yuba R Siwakoti, and Danda B Rawat. Phishing attack detection with ml-based siamese empowered orb logo recognition and ip mapper. In *Proc. of the IEEE INFOCOM Conference on Computer Communications Workshops*, 2022.

[60] Cheng Li, István Fehérvari, Xiaonan Zhao, Ives Macedo, and Srikanth Appalaraju. Seetek: Very large-scale open-set logo recognition with text-aware metric learning. In *Proc. of the IEEE/CVF Winter Conference on Applications of Computer Vision*, 2022.

[61] lindsey98/PhishingBaseline: Implementations of 3 phishing detection and identification baselines. (Accessed on 02/07/2024). URL: <https://github.com/lindsey98/PhishingBaseline>.

[62] Phishtank | join the fight against phishing. (Accessed on 10/30/2023). URL: <https://phishtank.org/>.

[63] Haijun Zhang, Gang Liu, Tommy W. S. Chow, and Wenyin Liu. Textual and visual content-based anti-phishing: A bayesian approach. *IEEE Transactions on Neural Networks*, 2011.

[64] Yannis Kalantidis, Lluis Garcia Pueyo, Michele Trevisiol, Roelof Van Zwol, and Yannis Avrithis. Scalable triangulation-based logo recognition. In *Proc. of the 1st ACM international conference on multimedia retrieval*, 2011.

[65] Flickr logos dataset | iva. (Accessed on 04/29/2024). URL: [http://image.ntua.gr/iva/datasets/flickr\\_logos/](http://image.ntua.gr/iva/datasets/flickr_logos/).

[66] Ee Hung Chang, Kang Leng Chiew, San Nah Sze, and Wei King Tiong. Phishing detection via identification of website identity. In *Proc. of the International Conference on IT Convergence and Security*, 2013.

[67] Stefan Romberg and Rainer Lienhart. Bundle min-hashing for logo recognition. In *Proc. of the 3rd ACM Conference on International Conference on Multimedia Retrieval*, 2013.

[68] Github - ankitnayan/bundle\_min\_hashing\_source: Implementation of bundle min hashing for logo recognition. (Accessed on 04/29/2024). URL: [https://github.com/ankitnayan/bundle\\_min\\_hashing\\_source](https://github.com/ankitnayan/bundle_min_hashing_source).

[69] Florian Schroff, Dmitry Kalenichenko, and James Philbin. Facenet: A unified embedding for face recognition and clustering. In *Proc. of the IEEE Conference on Computer Vision and Pattern Recognition*, 2015.

[70] Github - davidsandberg/facenet: Face recognition using tensorflow. (Accessed on 04/29/2024). URL: <https://github.com/davidsandberg/facenet>.

[71] Gary B Huang, Marwan Mattar, Tamara Berg, and Eric Learned-Miller. Labeled faces in the wild: A database for studying face recognition in unconstrained environments. In *Proc. of the Workshop on faces in 'Real-Life' Images: detection, alignment, and recognition*, 2008.

[72] Lior Wolf, Tal Hassner, and Itay Maoz. Face recognition in unconstrained videos with matched background similarity. In *Proc. of the IEEE conference on computer vision and pattern recognition*, 2011.

[73] Routhu Srinivasa Rao and Syed Taqi Ali. A computer vision technique to detect phishing attacks. In *Proc. of the International Conference on Communication Systems and Network Technologies*, 2015.

[74] Steven CH Hoi, Xiongwei Wu, Hantang Liu, Yue Wu, Huiqiong Wang, Hui Xue, and Qiang Wu. Logo-net: Large-scale deep logo detection and brand recognition with deep region-based convolutional networks. *arXiv preprint arXiv:1511.02462*, 2015.

[75] Ahmet Selman Bozkir and Ebru Akcapinar Sezer. Use of hog descriptors in phishing detection. In *Proc. of the International Symposium on Digital Forensic and Security (ISDFS)*, 2016.

[76] Shuichi Haruta, Hiromu Asahina, and Iwao Sasase. Visual similarity-based phishing detection scheme using image and css with target website finder. In *Proc. of the IEEE Global Communications Conference*, 2017.

[77] Rishabh Sharma and Anirudha Vishvakarma. Retrieving similar e-commerce images using deep learning. *arXiv preprint arXiv:1901.03546*, 2019.

[78] GitHub - khatria/Retrieving-Similar-E-Commerce-Images-Using-Deep-Learning: This repository is an implementation of the following research work using TensorFlow 2. (Accessed on 03/27/2024). URL: <https://github.com/khatria/Retrieving-Similar-E-Commerce-Images-Using-Deep-Learning>.

[79] Li Yuan, Tao Wang, Xiaopeng Zhang, Francis EH Tay, Zequn Jie, Wei Liu, and Jia Shi Feng. Central similarity quantization for efficient image and video retrieval. In *Proc. of the IEEE/CVF Conference on Computer Vision and Pattern Recognition*, 2020.

[80] GitHub - yuanli2333/Hadamard-Matrix-for-hashing: CVPR2020: Central Similarity Quantization/Hashing for Efficient Image and Video Retrieval. (Accessed on 03/27/2024). URL: <https://github.com/yuanli2333/Hadamard-Matrix-for-hashing>.

[81] Jia Deng, Wei Dong, Richard Socher, Li-Jia Li, Kai Li, and Li Fei-Fei. Imagenet: A large-scale hierarchical image database. In *Proc. of the IEEE conference on computer vision and pattern recognition*, 2009.

[82] S-Abdelnabi/VisualPhishNet. (Accessed on 02/07/2024). URL: <https://github.com/S-Abdelnabi/VisualPhishNet>.

[83] GitHub - d-li14/involution: [CVPR 2021] Involution: Inverting the Inherence of Convolution for Visual Recognition, a brand new neural operator. (Accessed on 03/27/2024). URL: <https://github.com/d-li14/involution>.

[84] Marius Cordts, Mohamed Omran, Sebastian Ramos, Timo Rehfeld, Markus Enzweiler, Rodrigo Benenson, Uwe Franke, Stefan Roth, and Bernt Schiele. The cityscapes dataset for semantic urban scene understanding. In *Proc. of the IEEE conference on computer vision and pattern recognition*, 2016.

[85] Bram van Dooremal, Pavlo Burda, Luca Alodi, and Nicola Zannone. Combining text and visual features to improve the identification of cloned webpages for early phishing detection. In *Proc. of the International Conference on Availability, Reliability and Security*, 2021.

[86] Bram van Dooremal, Pavlo Burda, Luca Alodi, and Nicola Zannone. Phishing website dataset, 2021. URL: <https://doi.org/10.5281/zenodo.4922598>.

[87] lindsey98/Phishpedia: Official Implementation of "Phishpedia: A Hybrid Deep Learning Based Approach to Visually Identify Phishing Webpages". (Accessed on 02/07/2024). URL: <https://github.com/lindsey98/Phishpedia>.

[88] Phishpedia: A Hybrid Deep Learning Based Approach to Visually Identify Phishing Webpages. (Accessed on 03/04/2024). URL: <https://sites.google.com/view/phishpedia-site/>.

[89] ucuapps. GitHub - ucuapps/OpenGlue: Open Source Graph Neural Net Based Pipeline for Image Matching, 2022. (Accessed on 03/27/2024). URL: <https://github.com/ucuapps/OpenGlue>.

[90] Zhengqi Li and Noah Snavely. Megadepth: Learning single-view depth prediction from internet photos. In *Computer Vision and Pattern Recognition (CVPR)*, 2018.

[91] neouyghur | metu-trademark-dataset. (Accessed on 04/29/2024). URL: <https://github.com/neouyghur/METU-TRADEMARK-DATASET>.

[92] mubastan/osld | Open Set Logo Detection Dataset (OSLD Dataset). (Accessed on 03/17/2024). URL: <https://github.com/mubastan/osld>.

[93] Ahmet Selman Bozkir and Murat Aydos. Logosense: A companion hog based logo detection scheme for phishing web page and e-mail brand recognition. *Computers & Security*, 2020.

## A APPENDIX

### A.1 Model Summary

We conduct a comprehensive literature review of top computer vision, security, and machine learning conferences to identify relevant visual similarity-based models for phishing detection. We selected six promising models to retrain and evaluate from this search in our study, as summarized in Table 7. The gray shading in the table indicates the six models selected for re-training and evaluation in our study.

The selected models span from 2005 to 2022 and employ diverse techniques for assessing websites' visual similarity. Liu *et al.* [53] compares features like layout, colors, fonts, and image placement, while EMD [6] uses Earth Mover's Distance to measure visual similarity. Medvet *et al.* [54], CCH [55], and Goldphish [56] analyze discriminative key points, employ image hashing techniques, and leverage machine learning classifiers for phishing detection, respectively. More recent approaches like Phishpedia [3] combine text and visual content analysis, while OpenGlue [33], Bernabeu *et al.* [57], OSLD [58], Bhurtel *et al.* [59], and SeeTek [60] explore advanced deep learning techniques for image retrieval, logo recognition, and visual similarity assessment. In particular, the use of deep learning

**Table 6: Failure Example Categorization.**

ID	Description
Logo	L1 Screenshot delete the logo
	L2 Different color of logo
	L3 Logo's ratio is changed
	L4 Logo is rotated in some angles
	L5 Logo is combined with other logos
	L6 Logo appear in different locations on the screenshot
	L7 Flipping logo by vertical or horizontal
	L8 The screenshot replaces the logo with other logos
	L9 The logo or screenshot is blurred
	L10 Screenshot with enlarged or shrunk logo
	L11 Only one part (text or image) is used if it has multiple parts
	L12 Logo font is changed
	L13 Text part is all or partially replaced with upper or lowercase
	L14 The logo is outdated
	L15 Design new logos based on the name or their original logo
	L16 Logo with different shapes, like square, rectangular
	L17 Change the test-logo language
Popup	P1 Login form pops up on the screenshot
	P2 Advertisements pop up on the screenshot
	P3 The cookie pop up on the blurred screenshot
	P4 Alert, remind, location, etc.
Login	F1 Change login form text (text, color, language, fonts)
	F2 Change button color, shape, location, text, etc.
	F3 Design a new form
	F4 Use other websites as login methods
	F5 Login by scanning QR code

(DL) techniques since 2019 shows a growing trend toward applying DL to visual similarity-based phishing detection.

## A.2 Selected Model

Based on the candidate papers, we carefully selected six models to comprehensively compare visual similarity-based phishing detection approaches, as detailed in Table 8. Our selection includes two deep learning models (*PhishIntention* [4] and *Phishpedia* [3]), which are specifically designed to identify phishing target brands through logo components. We also selected a deep-learning model that detects phishing using screenshots (*VisualPhishNet* [5]), and a deep-learning model (*Involution* [33]) not explicitly targeted to detect phishing, and two traditional machine learning approaches, *EMD* (Earth Mover's Distance) [6] for screenshot-based phishing detection and *PhishZoo* [8] for logo-based detection. Detailed model information can refer to Table 8.

By including models with diverse architectures, input types, and detection methods, we aim to provide insights into the strengths and limitations of various visual similarity-based phishing detection techniques. The detailed information for each selected model can be found in Table 8.

## A.3 Failure Examples Categorization

To better understand the limitations of visual similarity-based phishing detection models, we analyzed the failure cases observed during our real-world evaluations in Section 5. We categorized

these failure examples into three main categories: logo-related issues, popup-related issues, and login form-related issues, as summarized in Table 6. Logo-related issues (L1-L17) encompass various manipulations and alterations to the logo, such as deletion, color changes, ratio modifications, rotations, combinations with other logos, and placement in different locations on the screenshot. These issues highlight models' challenges in accurately identifying and comparing logos under diverse visual variations. Popup-related issues (P1-P4) pose a significant threat. They involve the presence of popups, advertisements, cookies, alerts, and other overlays on the screenshot. These elements can obstruct or confuse the visual analysis of the webpage, potentially leading to misclassifications by the phishing detection models and, consequently, to successful phishing attacks. Login form-related issues (F1-F5) include changes to the login form's text, color, language, font, and other website login forms as a phishing tactic. These variations in the login form's appearance and design can make it difficult for models to accurately identify phishing attempts based on visual similarity alone.

## A.4 Perturbed Logo Samples

To assess the robustness of phishing detection models against adversarial attacks, we introduce perturbations to the logos using popular white-box and black-box attack techniques. The perturbed logos are then returned to their original positions on the screenshots. We use Faster RCNN to crop the logos from the screenshots to evaluate whether the perturbed logos can evade detection by the object detection model. The perturbed logo samples, cropped by Faster RCNN, are shown in Figure 4. We apply six different attack methods:

- *Fast Gradient Sign Method (FGSM)* [41]: A white-box attack that adds perturbations to the logo based on the gradients of the target model, calculated in a single step.
- *Projected Gradient Descent (PGD)* [42]: An iterative version of the FGM attack, which applies the perturbations multiple times to create a more effective adversarial example.
- *Carlini & Wagner (CW)* [43]: A strong white-box attack that optimizes the perturbations to minimize the detection confidence of the target model.
- *Vision Transformer (ViT)* [44]: A transformer-based architecture for image classification that splits an image into patches and processes them using self-attention mechanisms.
- *Swin Transformer (Swin)* [45]: A hierarchical vision transformer that uses shifted window attention to capture both local and global dependencies in an image efficiently.
- *Style Retention Network (SRNet)* [35]: A generative adversarial network (GAN) that aims to transfer the style of one image to another while preserving the content of the target image.

## A.5 Examples of Visible Manipulation

Focusing on the logo component, we randomly sample the failure result and select some samples that can make models fail. We also selected the samples based on the manipulations used by the adversaries. Detailed examples can refer to Figure 5.

**Table 7: List of Visual Similarity-based Models (Y: open source code, N: no open source code, Y\*: reproduced by others).**

Year Model	Description	DL Code	Data Source
2005 Liu <i>et al.</i> [53]	Compares features like layout, colors, fonts, and image placement of webpages for phishing detection	N N	N
2006 EMD [6]	Uses Earth Mover's Distance to assess visual similarity of webpages for phishing detection	N Y* [61]	N
2008 Medvet <i>et al.</i> [54]	Relies on visual similarity, potentially comparing features like layout, colors, and overall webpage appearance, to detect phishing	N N	PhishTank [62], Alexa
2009 CCH [55]	Employs discriminative keypoint features to distinguish phishing websites based on visual cues	N N	N
2010 Goldphish [56]	Analyzes images for phishing detection, possibly using techniques like image recognition or text extraction from images	N N	PhishTank [62]
2011 Zhang <i>et al.</i> [63]	Combines textual and visual content analysis with a Bayesian approach for phishing detection	Y N	N
2011 msDT [64]	Introduces a method for logo recognition (not phishing specific) based on triangulation	N N	Flickr [65]
2011 PhishZoo [8]	Analyzes visual appearance of webpages, likely using techniques to compare layout, colors, fonts, and potentially images	N Y* [61]	PhishTank [62], Alexa
2013 Chang <i>et al.</i> [66]	Focuses on website identity recognition, possibly using techniques like domain name analysis or website structure comparison	N N	PhishTank [62], Alexa
2013 Romberg <i>et al.</i> [67]	Proposes bundle min-hashing for logo recognition	N Y [68]	Flickr [65]
2015 FaceNet [69]	Deep learning architecture for face recognition (not directly related to phishing)	Y Y [70]	LFW [71], YouTube [72]
2015 Rao <i>et al.</i> [73]	Presents a computer vision technique for phishing detection using visual similarity	N N	PhishTank [62]
2015 LOGO-Net [74]	Leverages deep learning for logo detection (not directly related to phishing)	Y N	N
2016 Bozkir <i>et al.</i> [75]	Uses HOG descriptors for feature extraction to potentially compare webpages for phishing detection	N N	N
2017 Haruta <i>et al.</i> [76]	Combines image and CSS analysis with a target website finder for phishing detection	N N	Alexa
2019 Sharma <i>et al.</i> [77]	Deep learning approach for image retrieval (adaptable to phishing)	Y Y [78]	N
2020 CSQ [79]	Deep learning method for image/video retrieval (adaptable to phishing)	Y Y [80]	ImageNet [81]
2020 VisualPhishNet [5]	Proposes zero-day phishing website detection based on visual similarity	Y Y [82]	N
2021 Involution [21]	Inverting the inherence of convolution for visual recognition	Y Y [83]	Cityscapes [84]
2021 Dooremael <i>et al.</i> [85]	Combining text and visual features to improve the identification of cloned webpages for early phishing detection	Y N	Dataset [86]
2021 Phishpedia [3]	Employs a hybrid deep learning approach for visual phishing detection	Y Y [87]	Phishpedia [88]
2022 PhishIntention [4]	Uses deep learning to analyze webpage appearance and dynamics for inferring phishing intention	Y Y [61]	PhishIntention [61]
2022 OpenGlue [33]	Open-source deep learning pipeline for image matching (not directly related to phishing)	Y Y [89]	MegaDepth [90]
2022 Bernabeu <i>et al.</i> [57]	Leverages deep learning for multi-label logo recognition (not directly related to phishing)	Y N	METU [91]
2022 OSLD [58]	Deep learning approach for large-scale logo detection (not directly related to phishing)	Y N	OSLD [92]
2022 Bhurtel <i>et al.</i> [59]	Relies on machine learning with a Siamese network for logo recognition for phishing detection	Y N	LogoSENSE [93]
2022 SeeTek [60]	Deep learning for large-scale logo recognition with text integration (not directly related to phishing)	Y N	PL8K

where deeper shades of  indicates the six models that we select for retraining and evaluation.

**Table 8: Description of Six Models Information Used in This Work.**

Model Name	Training Dataset	Input	Description
EMD [6]	—	S	Calculate screenshots' distance by EMD through color and coordinate feature
PhishZoo [8]	—	S, U, H	Use TF-IDF on URL and HTML for profile matching and use the SIFT feature for image matching
VisualPhishNet [5]	Extended Ref.	S	Use Triplet CNN to learn between same-website screenshots' similarity and dissimilarity between different-website screenshots.
Involution [21]	Logo2K+, PhishIntention Ref. or Extended Ref.	S	Use Faster RCNN find Logo region, learn logo representations through Involution, compare cosine similarity
Phishpedia [3]	Logo2K+, Benign30K, PhishIntention Ref. or Extended Ref.	S, U, H	Contains a layout classifier to find the logo region and a Siamese model to recognize the logo's brand
PhishIntention [4]	Logo2K+, Sampled Benign30K, PhishIntention Ref. or Extended Ref.	S, U, H	Contains a layout classifier part to find the different components' regions, a CRP classifier to check if the screenshot has CRP, HTML static classifier to check whether have CRP, a CRP locator to find additional links' CRP, and a siamese model to recognize the logo's brand

\*Testing Dataset = APWG Dataset, Manipulating Dataset; \*\*Brand Reference List = PhishIntention, Extended Reference List; S = Screenshot; U = URL; H = HTML;

**Figure 4: Perturbed Manipulation Samples Cropped by Faster RCNN.**

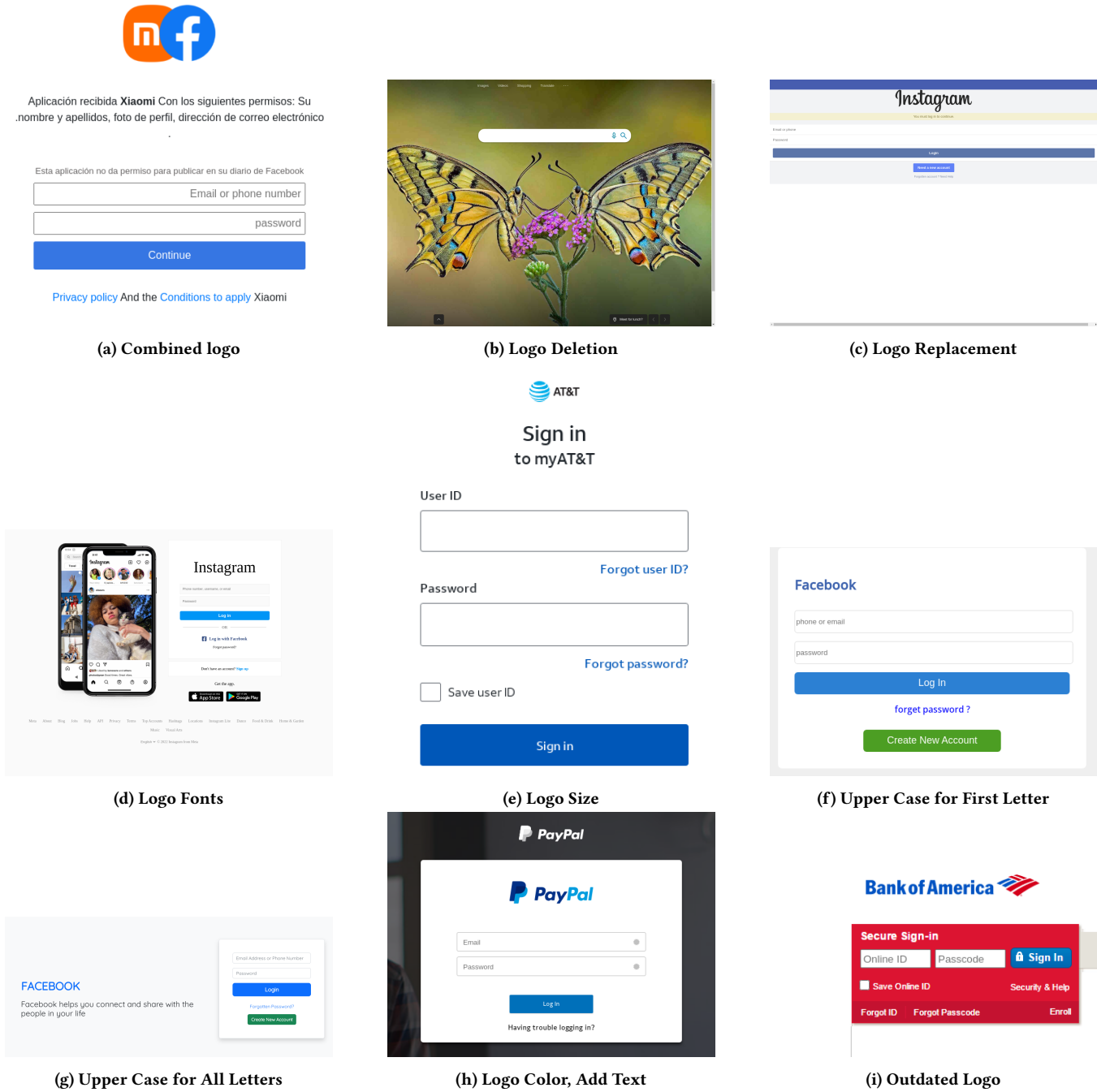


Figure 5: Examples of Manipulated Samples Found in Our Real-world Phishing Dataset.